Spatial and diurnal variability in reactive nitrogen oxide chemistry as reflected in the isotopic composition of atmospheric nitrate: Results from the CalNex 2010 field study

W. C. Vicars, Samuel Morin, J. Savarino, N. L. Wagner, J. Erbland, E. Vince, J. M. F. Martins, B. M. Lerner, P. K. Quinn, D. J. Coffman, et al.

Spatial and diurnal variability in reactive nitrogen oxide chemistry as reflected in the isotopic composition of atmospheric nitrate: Results from the CalNex 2010 field study

W. C. Vicars,[1,2] S. Morin,[3] J. Savarino,[1] N. L. Wagner,[4,5] J. Erbland,[1] E. Vince,[6] J. M. F. Martins,[6] B. M. Lerner,[4,5] P. K. Quinn,[7] D. J. Coffman,[7] E. J. Williams,[4,5] and S. S. Brown[4]

Received 5 November 2012; revised 17 July 2013; accepted 21 July 2013; published 17 September 2013.

[1] Here we present measurements of the size-resolved concentration and isotopic composition of atmospheric nitrate (NO_3^-) collected during a cruise in coastal California. Significant differences in air mass origin and atmospheric chemistry were observed in the two main regions of this cruise (South and Central Coast) with corresponding differences in NO_3^- concentration and isotope ratios. Measurements of the ^{17}O-excess ($\Delta^{17}O$) of NO_3^- suggest that nocturnal chemistry played an important role in terms of total NO_3^- production (~ 50%) in the coastal Los Angeles region (South Coast), where NO_3^- concentrations were elevated due to the influence of sea breeze / land breeze recirculation and $\Delta^{17}O(NO_3^-)$ averaged (25.3 ± 1.6)‰. Conversely, $\Delta^{17}O(NO_3^-)$ averaged (22.3 ± 1.8)‰ in the Central Coast region, suggesting that the daytime OH + NO_2 reaction was responsible for 60–85% of NO_3^- production in the marine air sampled in this area. A strong diurnal signal was observed for both the $\Delta^{17}O$ and $\delta^{15}N$ of NO_3^-. In the case of $\Delta^{17}O$, this trend is interpreted quantitatively in terms of the relative proportions of daytime and nighttime production and the atmospheric lifetime of NO_3^-. For $\delta^{15}N$, which had an average value of (0.0 ± 3.2)‰, the observed diurnality suggests a combined effect of isotopic exchange between gas-phase precursors and variability in reactive nitrogen sources. These findings represent a significant advance in our understanding of the isotope dynamics of nitrate and its precursor molecules, with potentially important implications for air quality modeling.

Citation: Vicars, W. C., et al. (2013), Spatial and diurnal variability in reactive nitrogen oxide chemistry as reflected in the isotopic composition of atmospheric nitrate: Results from the CalNex 2010 field study, *J. Geophys. Res. Atmos.*, *118*, 10,567–10,588, doi:10.1002/jgrd.50680.

1. Introduction

[2] Reactive nitrogen oxides ($NO + NO_2 = NO_x$) exert a significant influence on the chemistry of the troposphere through the catalysis of photochemical ozone production and are closely coupled with air quality and atmospheric oxidative capacity (i.e., the lifetime of organic compounds from oxidation by radicals) [*Monks*, 2005]. The quantification of NO_x emissions and the elucidation of its subsequent chemical transformation pathways are thus topics of considerable current interest [*Ryerson et al.*, 2013]. NO_x is present in the troposphere as a result of several natural processes, including biogeochemical cycling in soils (i.e., nitrification and denitrification), conversion from inert N_2 gas by lightning, and downward transport from the stratosphere. However, the global tropospheric NO_x budget is currently dominated by anthropogenic activities, with fossil fuel combustion accounting for approximately 60% of global NO_x emissions [*Jaegle et al.*, 2005].

[3] Nitrate, defined in the present study as the sum of gaseous nitric acid (HNO_3) and particulate NO_3^-, is the major oxidation product of NO_x in the atmosphere. Due to its exceptionally high solubility in water, nitrate is rapidly deposited upon formation onto surfaces and in water droplets, with a lifetime against deposition ranging from several hours to ~ 1 day for gaseous HNO_3 [*Liang et al.*, 1998; *Brown et al.*, 2004] and from several days to one week for particulate nitrate present in the accumulation mode [*Millet et al.*, 2004].

Additional supporting information may be found in the online version of this article.

[1]LGGE, UMR 5183, UJF-Grenoble 1/CNRS, Grenoble, France.
[2]Now at Institute of Alpine and Arctic Research, University of Colorado Boulder, Boulder, Colorado, USA.
[3]Météo-France - CNRS, CNRM-GAME UMR 3589, CEN, Grenoble, France.
[4]NOAA Earth Systems Research Laboratory, Boulder, Colorado, USA.
[5]Cooperative Institute for Research in Environmental Sciences, University of Colorado Boulder, Boulder, Colorado, USA.
[6]LTHE, UMR 5564, UJF-Grenoble 1/CNRS-INSU/G-INP/IRD, Grenoble, France.
[7]NOAA Pacific Marine Environmental Laboratory, Seattle, Washington, USA.

Corresponding author: W. C. Vicars, Institute of Alpine and Arctic Research, University of Colorado Boulder, 1560 30th St., Boulder, CO 80303, USA. (william.c.vicars@colorado.edu)

2169-897X/13/10.1002/jgrd.50680

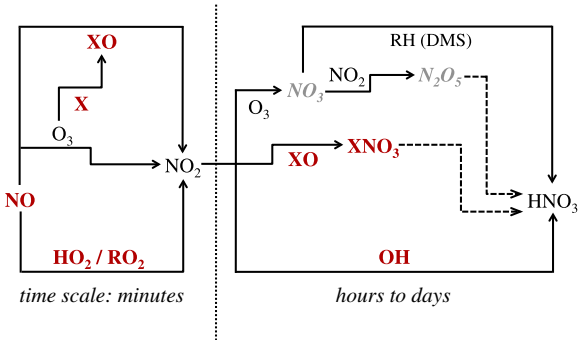

Figure 1. An overview of the major processes leading to the conversion of NO_x to nitrate in the troposphere. Nitrate precursor gases associated with daytime and nighttime pathways are indicated by bold (red) and italicized (grey) text, respectively. Dashed lines indicate heterogeneous surface reactions on atmospheric particles.

These dry and wet deposition processes represent environmentally significant nitrogen input pathways and have been intensively studied with regards to their role in the eutrophication of aquatic ecosystems and the acidification of soils and surface waters [*Likens et al.*, 1996; *Holland et al.*, 1997; *Fenn et al.*, 2003]. Some recent studies of nitrate deposition have focused on the extraction of quantitative information regarding NO_x sources and cycling in the troposphere [*Elliott et al.*, 2007; *Costa et al.*, 2011]; because nitrate is one of the most abundant ions present in polar ice and snow, there also exists the possibility of extending these atmospheric interpretations based on nitrate into the past using ice cores [*Alexander et al.*, 2004; *Hastings et al.*, 2009].

[4] Figure 1 summarizes the essential features of the NO_x cycle leading to nitrate formation in the troposphere. During the day, NO and NO_2 interconvert through the photochemical NO_x cycle, in which NO_2 undergoes photolysis to form NO (R1), generating atomic oxygen that may subsequently combine with molecular oxygen to form ozone (R2) [*Crutzen*, 1970]:

$$NO_2 + h\nu \rightarrow NO + O \quad \text{(R1)}$$

$$O + O_2 + M \rightarrow O_3 + M \quad \text{(R2)}$$

$$O_3 + NO \rightarrow NO_2 + O_2 \quad \text{(R3)}$$

$$HO_2 + NO \rightarrow NO_2 + OH \quad \text{(R4)}$$

$$RO_2 + NO \rightarrow NO_2 + RO \quad \text{(R5)}$$

$$XO + NO \rightarrow NO_2 + X \quad \text{(R6)}$$

[5] The NO resulting from the (R1) pathway reacts rapidly to reform NO_2, primarily through oxidation by ozone (R3) or peroxy radicals, HO_2/RO_2 ((R4)/(R5)), although reactive halogen oxides (XO = BrO, ClO, IO, etc.) may also participate in NO oxidation in some cases (R6) [*Stutz et al.*, 1999; *Platt and Hönninger*, 2003; *von Glasow et al.*, 2004]. Cycling between NO and NO_2 occurs so rapidly that a steady state is established during the day ("photostationary state"); conversely, the processes leading to the conversion of NO_2 to nitrate operate on time scales at least 3 orders of magnitude longer [*Atkinson et al.*, 2004]:

$$NO_2 + O_3 \rightarrow NO_3 + O_2 \quad \text{(R7)}$$

$$NO_2 + OH + M \rightarrow HNO_3 + M \quad \text{(R8)}$$

$$NO_2 + XO + M \rightarrow XNO_3 + M \quad \text{(R9)}$$

$$XNO_3 + H_2O_{(liquid)} \rightarrow HOX + HNO_{3\ (aq)} \quad \text{(R10)}$$

[6] NO_2 is oxidized primarily by ozone (R7) or the hydroxyl radical (OH) (R8). Halogen oxides (e.g., BrO) are also thought to play a role in NO_2 oxidation, which can lead to nitrate formation through the hydrolysis of XNO_3 intermediates (R10) [*Sander et al.*, 1999]. However, both the (R6) and (R10) pathways are typically difficult to assess due to a lack of observational constraints on halogen activity in the ambient troposphere [*Alexander et al.*, 2009].

[7] The nitrate radical (NO_3), the product of the (R7) reaction, has an exceedingly short lifetime from photolysis and generally reaches significant concentrations only during the night; therefore, reaction with OH (R8) is the principal nitrate production channel operating during daylight hours. During the night, the NO_3 radical is converted to nitrate through reactions with hydrocarbons (RH), principally dimethyl sulfide (DMS) in marine or coastal regions [*Stark et al.*, 2007], and with NO_2 to produce dinitrogen pentoxide (N_2O_5):

$$NO_3 + RH(DMS) \rightarrow HNO_3 + \text{products} \quad \text{(R11)}$$

$$NO_3 + NO_2 \leftrightarrow N_2O_5 \quad \text{(R12)}$$

[8] N_2O_5 is an important intermediate in the NO_x cycle that can hydrolyze to form HNO_3 through heterogeneous reactions on the surface of aerosol particles:

$$N_2O_5 + H_2O_{(liquid)} \rightarrow 2HNO_{3\ (aq)} \quad \text{(R13)}$$

[9] This N_2O_5 loss pathway represents a significant nocturnal sink of NO_x and a source of aerosol. However, N_2O_5 may act as only a temporary NO_x reservoir, eventually

decomposing to reform NO_2 and NO_3 via (R12). The actual efficiency of N_2O_5 uptake and nitrate yield, which depends strongly on aerosol composition and meteorological conditions, remains an area of significant uncertainty [*Bertram and Thornton*, 2009; *Chang et al*., 2011]. Furthermore, the heterogeneous chemistry of N_2O_5 on chloride-containing aerosol, first identified in laboratory studies over two decades ago [*Finlayson-Pitts et al*., 1989], has only recently been shown to efficiently release reactive chlorine species to the atmosphere [*Osthoff et al*., 2008; *Thornton et al*., 2010]:

$$N_2O_5 + Cl^-_{(aq)} \rightarrow ClNO_2 + NO_3{}^-_{(aq)} \qquad \text{(R14)}$$

[10] Most previous studies of nocturnal NO_x transformations have assumed that N_2O_5 reactions on particles proceed solely through the hydrolysis channel to form two HNO_3 molecules. However, reaction with Cl^- may compete with N_2O_5 hydrolysis in the case of marine aerosols, with recent studies suggesting that this pathway represents a significant fraction of total N_2O_5 consumption in some polluted coastal environments [*Phillips et al*., 2012]. This N_2O_5 loss mechanism has important implications for air quality because it results in the production of nitryl chloride ($ClNO_2$) and only one HNO_3 molecule, thereby decreasing the magnitude of the nocturnal NO_x sink from HNO_3 formation while also forming a reactive halogen species that may subsequently influence ozone chemistry [*Sarwar et al*., 2012].

[11] Recently, there has been considerable interest in the use of nitrate stable isotope ratios as interpretive tools to identify sources of NO_x and to quantify and constrain the relative rates of NO_x removal mechanisms (i.e., the principal nitrate formation reactions: (R8), (R10), (R11), and (R13)) [*Michalski et al*., 2003; *Morin et al*., 2007, 2008; *Alexander et al*., 2009]. Stable isotope measurements are reported as isotopic enrichments (δ) relative to a standard reference material:

$$\delta = \frac{R_{\text{sample}}}{R_{\text{reference}}} - 1 \qquad (1)$$

where R represents the elemental $^{17}O/^{16}O$, $^{18}O/^{16}O$, or $^{15}N/^{14}N$ ratio in the sample and reference material, respectively. The reference used for oxygen isotope analysis is standard mean ocean water (SMOW), and the reference for nitrogen is atmospheric N_2. For practical reasons, δ values are typically reported in per mill (‰), as variations in isotopic ratios for natural samples occur within a very narrow range.

[12] Nitrogen isotope ratios ($\delta^{15}N$) of nitrate are typically thought to convey information regarding NO_x sources [*Russell et al*., 1998; *Hastings et al*., 2003; *Elliott et al*., 2007, 2009; *Morin et al*., 2009], although some previous studies have emphasized the role of kinetic fractionation effects [*Freyer*, 1991] and isotope exchange reactions [*Freyer et al*., 1993]. Conversely, the oxygen isotopic composition of nitrate ($\delta^{17}O$, $\delta^{18}O$) is usually interpreted in terms of the relative activities of different NO_x oxidation pathways [*Michalski et al*., 2003; *Alexander et al*., 2009; *Morin et al*., 2011]. The unique and distinctive ^{17}O-excess ($\Delta^{17}O$) of ozone (O_3) has been found to be a particularly useful isotopic fingerprint in studies of NO_x transformations. Ozone's anomalous isotopic composition arises due to non-mass-dependent fractionation during its formation in the atmosphere and results in an excess of ^{17}O over what is expected based on the abundance of ^{18}O (we define this quantity in the present paper in its linearized form as follows: $\Delta^{17}O = \delta^{17}O - 0.52 \times \delta^{18}O$) [*Thiemens*, 1999, 2006]. The $\Delta^{17}O$ signature of ozone is transferred to NO_x through oxidation reactions such that the $\Delta^{17}O$ of nitrate acts as a marker of the influence of ozone in its chemical formation (i.e., NO_x transformation pathway). This isotopic fingerprint, although it is subject to dilution, cannot be removed or altered via subsequent mass-dependent fractionation processes and is thus conserved during atmospheric transport and processing [*Brenninkmeijer et al*., 2003].

[13] The oxidative cycle shown in Figure 1 results in varying degrees of $\Delta^{17}O$ transfer depending on the relative importance of the different oxidants involved in nitrate production. Nighttime reactions involving the NO_3 radical lead to the formation of a nitrate product with a relatively high $\Delta^{17}O$ inherited from ozone; conversely, the daytime production of nitrate leads to a lesser $\Delta^{17}O$ transfer as the photochemically produced radicals (OH, HO_2, RO_2) involved in the NO_x cycle posses negligible ^{17}O-excess [*Dubey et al*., 1997; *Savarino and Thiemens*, 1999; *Lyons*, 2001; *Zahn et al*., 2006]. This disproportionality in isotope transfer provides a unique approach for tracing the chemical oxidation of gas-phase nitrate precursors, a technique that has been particularly effective in studies of NO_x cycling in the polar atmosphere where the occurrence of continuous sunlight during the summer (polar day) and continuous darkness during the winter (polar night) leads to pronounced seasonal differences in atmospheric chemistry [*Michalski et al*., 2005; *McCabe et al*., 2007; *Savarino et al*., 2007; *Morin et al*., 2007, 2008, 2012; *Frey et al*., 2009; *Erbland et al*., 2013]. $\Delta^{17}O(NO_3^-)$ measurements have also allowed for the analysis of seasonal variations in NO_x transformation dynamics occurring in the midlatitude and tropical troposphere [*Hastings et al*., 2003; *Michalski et al*., 2003; *Morin et al*., 2009]. However, while interpretations derived from nitrate isotope ratios have proven useful in the analysis of annual and seasonal atmospheric trends, any potential isotopic effects associated with more rapid changes in atmospheric chemistry (e.g., diurnal variations) are presently not well documented. Diurnal fluctuations in $\Delta^{17}O(NO_3^-)$, which should be present only when the atmospheric lifetime of nitrate is sufficiently short to allow for their development, are expected to reflect the relative activities of nighttime and daytime nitrate production pathways [*Morin et al*., 2011]. The $\Delta^{17}O$ of atmospheric nitrate may thus provide a tracer for the magnitude of the nocturnal NO_x sink in different atmospheric contexts. This could be a particularly useful tool, as the role played by nocturnal oxidation pathways in the transformation and removal of NO_x emissions is an area of significant uncertainty and it is unclear to what extent current regional models accurately represent these processes and their impact on air quality [*Brown et al*., 2004, 2006]. However, the sensitivity of $\Delta^{17}O(NO_3^-)$ to diurnal variations in NO_x oxidation pathways has yet to be established in field studies.

[14] In this study, measurements of the mass concentration and isotopic composition of atmospheric nitrate are reported for size-segregated aerosol samples collected during a research cruise along the coast of California. This cruise was

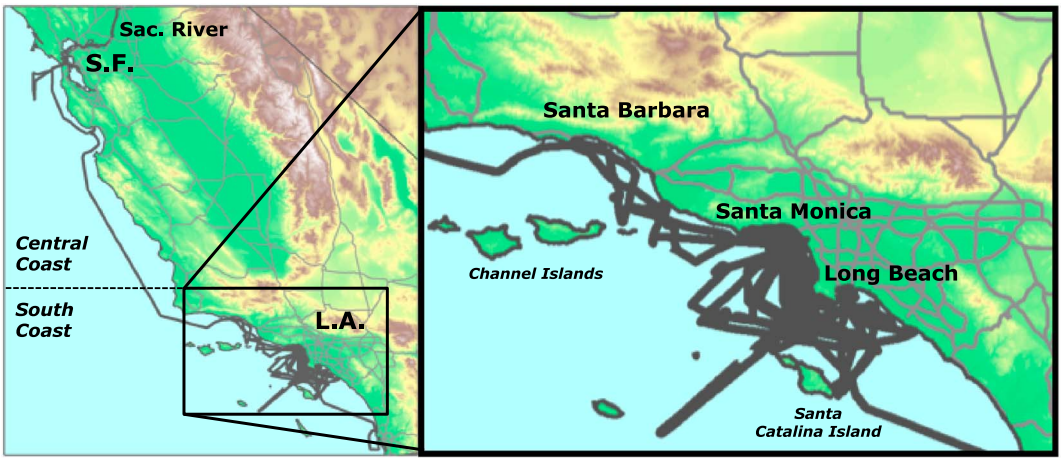

Figure 2. Map of California showing the cruise track (black lines) of the R/V *Atlantis* in relation to the geographical features discussed in the text.

organized as a component of the CalNex 2010 field study, a major multiagency campaign focusing on the atmospheric processes determining air quality over California and the eastern Pacific coastal region [*Ryerson et al*., 2013]. Aerosol sampling was conducted on a 12 h frequency for much of the cruise, allowing for direct daytime/nighttime comparisons and providing an opportunity to extract quantitative information regarding the temporal evolution of nitrate stable isotope ratios. Furthermore, samples were collected under two distinct transport regimes, allowing for an evaluation of the differences in NO_x transformation pathways occurring in air masses of marine and continental origin. This study, to the best of our knowledge the first of its kind, represents a significant advance in our understanding of the factors controlling the isotopic composition of atmospheric nitrate, with potentially important implications for air quality modeling.

2. Methods

2.1. High-Volume Air Sampling

[15] Sampling was conducted onboard the research vessel (R/V) *Atlantis* during a cruise along the coast of California (32.8°N–38.6°N) throughout the period 14 May–7 June 2010 (Figure 2) (see *Ryerson et al*. [2013] for details of the CalNex 2010 campaign). Atmospheric aerosol samples were collected onboard the R/V *Atlantis* using a high-volume air sampler (HVAS), which was operated at various sampling durations ranging from 2 to 22 h. The HVAS draws air at a flow rate of 1.1 $m^3\,min^{-1}$ through a four-stage cascade impactor (Tisch Series 230), which was loaded with slotted glass fiber filters (Tisch TE-230GF, 12.7 × 17.8 cm) and a larger glass fiber backup filter (Whatman GF/A, 20.3 × 25.4 cm). All glass fiber filters were cleaned before sampling by rinsing 3 times with ultrapure water. The cascade impactor aerodynamically fractionates bulk aerosol into five particle size classes with cuts at 7.2, 3.0, 1.5, 0.95, and 0.49 μm aerodynamic diameter (D_a). In order to ensure an amount of nitrate sample sufficient for isotopic analysis in each extract solution (approximately 100 nmol), the filters of the first three stages and those of the last two stages were combined into two separate samples, one comprised of the total supermicron ("coarse fraction," $D_a > 0.95$ μm) particle fraction and the other containing all submicron ("fine fraction," $D_a < 0.95$ μm) particles [*Baker et al*., 2007].

[16] The exact nature of the nitrate species collected during sampling using glass fiber filters has always been an area of some debate due primarily to (i) the likelihood of gaseous HNO_3 adsorption onto the aerosol particles already captured within the filter material and (ii) the disassociation and subsequent evaporative loss of NH_4NO_3 [see *Yeatman et al*., 2001, and references therein]. In this study, we have assumed that the HVAS filters quantitatively collect both particulate bound nitrate and gaseous HNO_3, which is likely considering the high sea-salt content of the marine boundary layer (MBL) [*Prospero and Savoie*, 1989]. This approach is identical to that adopted by *Morin et al*. [2009] in a previous sampling campaign using the HVAS in the Atlantic MBL; furthermore, it is consistent with most previous studies of atmospheric nitrate isotopes at coastal sites [*Michalski et al*., 2003; *Morin et al*., 2007; *Patris et al*., 2007; *Savarino et al*., 2007], thus insuring that the results obtained here are intercomparable with those reported in the literature. In the case of size-segregated measurements, we assume that gaseous HNO_3 was sampled together with submicron aerosol nitrate on the backup filter, consistent with *Morin et al*. [2009].

[17] A total of 63 sets of coarse and fine aerosol samples were collected during the cruise. The first 27 sets of samples, obtained during the period 14 May–27 May in the South Coast region (Figure 2), were collected on a diurnal frequency, from approximately 08:00–19:00 and 19:00–08:00 Pacific Standard Time (PST) for daytime and nighttime collections, respectively. Sampling durations were allowed to vary in the range of 3–22 h for the subsequent collection periods in the South Coast region during the period 28 May–31 May ($n = 12$). For the remainder of the cruise (1–7 June), the R/V *Atlantis* transited through the San Francisco Bay and the Sacramento River (Central Coast) where an additional 24 sets of HVAS samples were collected with sampling durations in the range of 2–12 h. In addition to the aerosol samples, seven sets of operational blanks were collected at regular intervals throughout the cruise. Blank filters were subjected to all of the same storage, handling, and

analytical procedures as field samples. After sampling, the filters were folded, placed into plastic bags, and stored in a freezer at −20°C. Samples were then transported frozen to Grenoble for further processing.

2.2. Nitrate Extraction and Chemical Analysis

[18] Aerosol filter samples were extracted in 40 mL of UV-oxidized deionized water (18.2 MΩ resistivity), and the extract solutions were then filtered via centrifugation using Millipore Centricon™ filter units. Extract nitrate concentrations were then determined colorimetrically using a segmented-flow analyzer (QuAAtro™, SEAL Analytical). In this technique, nitrate was quantitatively reduced to nitrite by passage through a column containing copperized cadmium. The resulting nitrite was then determined by diazotization with sulfanilamide dihydrochloride followed by detection of absorbance at 520 nm, a technique with a measurement uncertainty of approximately ± 2% [*Patey et al*., 2008]. Samples were calibrated against nitrate standards obtained from the National Institute of Standards and Technology. Atmospheric nitrate concentrations were calculated as the quotient of nitrate filter loading and the total volume of air pumped through the filter at standard temperature and pressure. The nitrate contribution from blank filters was almost always found to be negligible (< 5% of sample nitrate concentration for all samples with isotopic values reported in this study).

2.3. Isotopic Analysis

[19] Isotope ratios of nitrate ($^{17}O/^{16}O$, $^{18}O/^{16}O$, and $^{15}N/^{14}N$) were measured on a Finnigan™ MAT253 isotope ratio mass spectrometer (IRMS), which was equipped with a GasBench II™ online gas introduction system and coupled to an in-house built nitrate interface. Nitrate in the HVAS filter extracts was prepared for isotopic analysis by conversion to N_2O via the bacterial denitrifier method [*Sigman et al*., 2001; *Casciotti et al*., 2002; *Kaiser et al*., 2007]. The details of our analytical procedure are well described in the literature (for example, by *Morin et al*. [2009]) and will be only briefly outlined here.

[20] Denitrifying bacteria (*Pseudomonas aureofaciens*) were cultured in nitrate-amended soy broth and incubated for 5 days in stoppered glass bottles. Bacterial cultures, after concentration by centrifugation and resuspension, were dispensed as 2 mL aliquots into 20 mL glass vials, which were then crimped and purged with helium for 3 h. Approximately 100 nmol of sample nitrate was then injected into the purged vials, and the conversion of nitrate to nitrous oxide (N_2O) via bacterial denitrification was allowed to proceed overnight. The N_2O produced via denitrification was then cryofocused in a liquid nitrogen trap and introduced into a gold furnace where it was thermally decomposed at 900°C to O_2 and N_2. Following separation via gas chromatography, the O_2 and N_2 sample gases were directed into the ionization chamber of the IRMS. All analytical steps were simultaneously performed on 100 nmol of nitrate isotopic standards and their equimolar mixtures (International Atomic Energy Agency USGS 32, USGS 34, and USGS 35) [*Michalski et al*., 2002; *Böhlke et al*., 2003; *Brand et al*., 2009]. Individual analyses were normalized through comparison with these three nitrate reference materials. The overall accuracy of the method is estimated as the reduced standard deviation of the residuals from the linear regression between the measured reference materials and their expected values. For the results described here, the highest uncertainty values obtained for $\delta^{18}O$, $\Delta^{17}O$, and $\delta^{15}N$ were 2.0‰, 0.43‰, and 0.46‰, respectively.

2.4. Complementary Data

[21] In order to establish the dominant routes of atmospheric transport during the cruise, air mass back trajectory analysis was conducted using the NOAA HYSPLIT (hybrid single-particle Lagrangian integrated trajectory) model [*Draxier and Hess*, 1998]. A 5 day back trajectory was computed for each sampling midpoint at an arriving altitude of 100 m above sea level. The position of arrival for each trajectory was set to match the geographical location of the ship at the midpoint of each sampling period.

[22] In addition to the HVAS, the R/V *Atlantis* also carried an assortment of instrumentation for in situ measurements of trace gases (e.g., O_3 and NO_x), spectrally resolved irradiance (e.g., $j(O^1D)$ and $j(NO_2)$), aerosol physical and chemical properties, and meteorological variables (e.g., temperature, wind speed, and relative humidity) [*Ryerson et al*., 2013]. One minute average NO_x concentrations were determined via ozone-induced chemiluminescence/LED photolysis with a reported uncertainty of ± 4% and ± 11% for NO and NO_2, respectively [*Lerner et al*., 2009]. Ozone was measured continuously using a standard UV-absorption technique with a reported uncertainty of ± 2% [*Williams et al*., 2006]. Additionally, in situ measurements of N_2O_5 were obtained via Cavity Ring-Down Spectroscopy (CaRDS). The CaRDS instrument detects N_2O_5 by thermal conversion to NO_3 followed by detection of absorbance at 662 nm. N_2O_5 was measured at 1 min sampling durations throughout the cruise with a reported uncertainty of ± 10% [*Wagner et al*., 2011]. Aerosol size distributions were determined using an integrated system of Aitken DMPS (Differential Mobility Particle Sizer), accumulation mode DMPS, and APS (Aerodynamic Particle Sizer) instrumentation [*Bates et al*., 2005].

3. Results

[23] The following section presents time series of the concentration and stable isotope ratios of atmospheric nitrate collected throughout the R/V *Atlantis* cruise. This approach in displaying the results has been adopted in order to emphasize the diurnal variations observed. However, it should be kept in mind that these are not strictly temporal variations due to the movement of the ship. Nevertheless, these spatial variations were limited within the two major regions of sampling (South Coast and Central Coast, Figure 2); therefore, we have presented our measurements as a function of time but have made an effort to differentiate between the two regions, which were found to have distinct characteristics in terms of air mass history, gas-phase chemistry, and nitrate concentration and isotopic composition. Results for atmospheric nitrate are first presented in their raw size-segregated form in order to highlight variations observed as a function of aerosol size. Subsequently, results are presented in bulk form by mass-weighting the results obtained for the different size fractions. This has been done to allow for the comparison of our data to previous measurements of nitrate isotopic composition, which have most often been performed on bulk

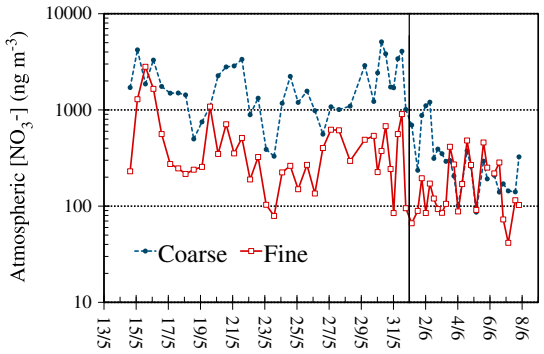

Figure 3. Temporal variability in the atmospheric concentration of nitrate in the coarse (supermicron) and fine (submicron) particle fractions. The solid black line indicates the period of transit between the South and the Central Coast regions (1 June).

aerosol samples [*Michalski et al.*, 2003; *Morin et al.*, 2007, 2008; *Savarino et al.*, 2007].

3.1. Atmospheric Nitrate Concentration and Complementary Data

[24] Variations in the concentration of atmospheric nitrate in the coarse ($D_a > 0.95$ µm) and fine ($D_a < 0.95$ µm) particle fractions are shown in Figure 3. Nitrate concentrations varied over a wide range during the cruise, with bulk values as high as 5 µg m^{-3} measured in the Santa Monica Bay (15–16 May and 30–31 May) and values as low as 150 ng m^{-3} in the San Francisco Bay area. In agreement with previous studies of nitrate particle size distributions in the MBL [*Yeatman et al.*, 2001; *Virkkula et al.*, 2006; *Arnold and Luke*, 2007; *Morin et al.*, 2009], nitrate was consistently enriched in the coarse fraction, with (mean ± 1σ) atmospheric concentrations of (1282 ± 1204) and (366 ± 434) ng m^{-3} for the coarse and fine fractions, respectively. The proportion of nitrate in the fine particle fraction varied in the range of 5–67% throughout the cruise, with a mean value of (27 ± 17)%.

[25] Clear differences in atmospheric nitrate concentration were observed between the South and Central Coast portions of the campaign. For the Central Coast, total atmospheric nitrate averaged (525 ± 321) ng m^{-3}, a range of values that is typical of the Pacific coastal MBL in areas not directly impacted by anthropogenic emissions [*Malm et al.*, 2004; *Patris et al.*, 2007]. Conversely, the South Coast region was characterized by elevated concentration, with an average of (2388 ± 1438) ng m^{-3}. This observation can be unambiguously attributed to differences in atmospheric transport pathways between the two regions: the results of 5 day back trajectory runs (Figure 4) indicate that the air masses reaching the South Coast region frequently arrived from a northerly or northeasterly direction, often passing over the Los Angeles metropolitan area en route (Figure 4a). These air masses typically transport large quantities of anthropogenic aerosol due to the influence of urban emissions in the South Coast air basin [*California Air Resources Board* (*CARB*), 2009]. Samples obtained in the Central Coast region were collected

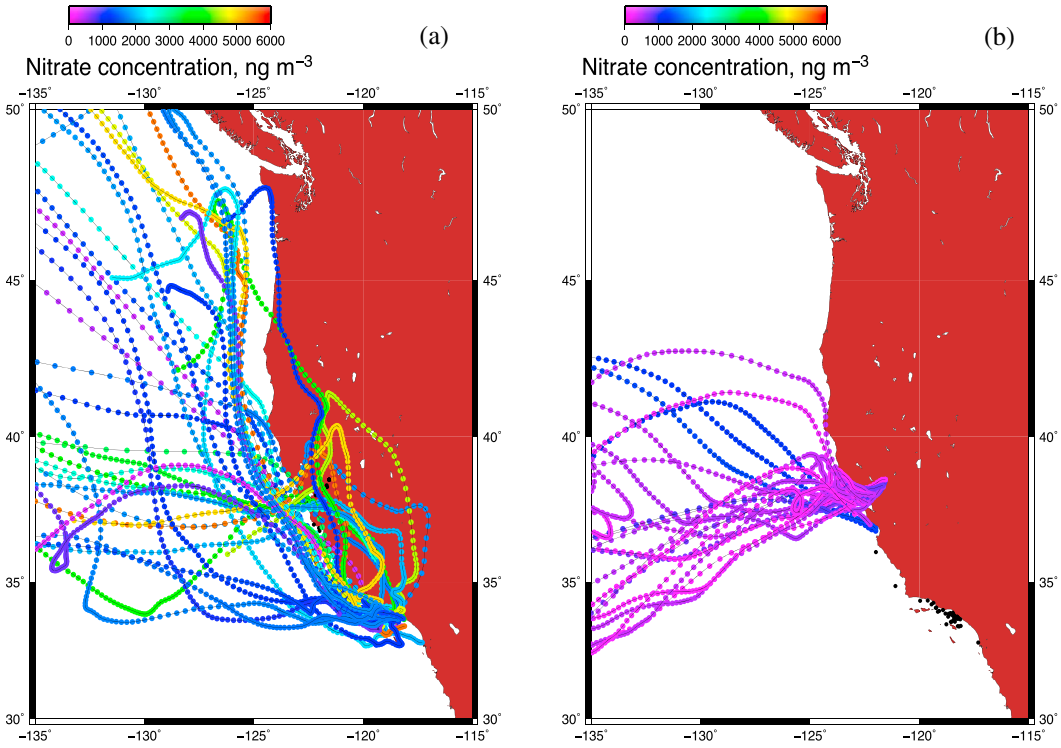

Figure 4. Backward trajectories of the air masses reaching the R/V *Atlantis* during the (a) South Coast and (b) Central Coast segments of the cruise. Back trajectory data were obtained from the National Oceanic and Atmospheric Administration (NOAA) GDAS database using the hybrid single-particle Lagrangian integrated trajectory (HYSPLIT) model [*Draxier and Hess*, 1998]. The trajectories are color coded based on the average concentration of atmospheric nitrate during each sampling period.

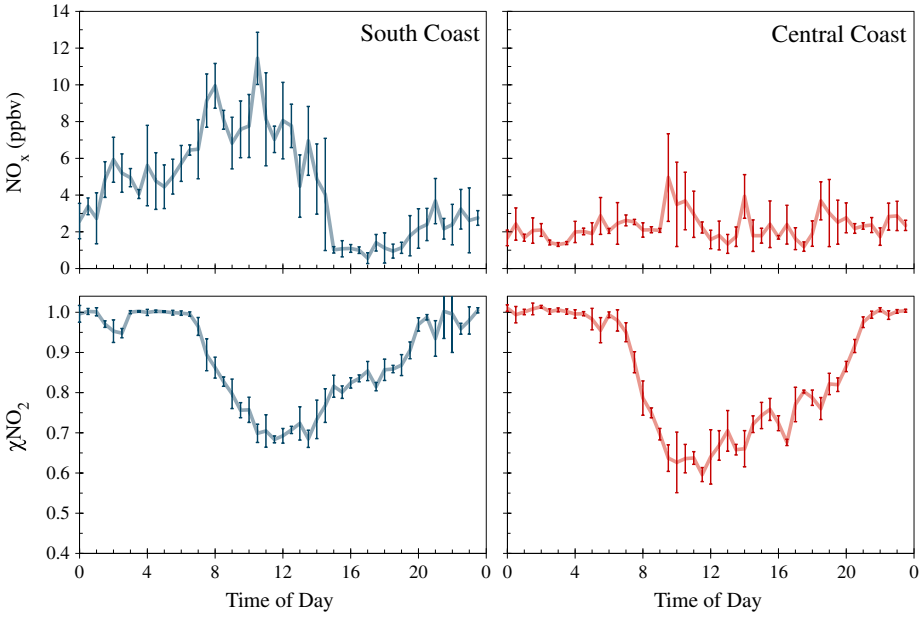

Figure 5. Diurnally averaged values for total NO_x concentration ($NO_x = NO + NO_2$) during the two major segments of the cruise on R/V *Atlantis* (upper panels). The values shown were computed by binning the 30 min averages of the NO and NO_2 concentration measurements conducted onboard. Error bars represent the standard deviation of the NO_x measurements in each of the individual 30 min time bins. The NO_2 molar ratio ($\chi NO_2 = NO_2/NO_x$) and its standard deviation are shown for each time bin in the lower panels.

from marine air masses arriving almost exclusively from a westerly or southwesterly direction (Figure 4b). The impact of air mass history is evident not only in the concentration of atmospheric nitrate but also in its distribution between the coarse and fine aerosol fractions. The proportion of nitrate in the coarse aerosol fraction was significantly higher (*t* tests have been used to constrain the significance of the differences, p much less than 0.001) in the South Coast region, whereas no statistically significant difference was detected between size fractions in the Central Coast ($p > 0.001$). In agreement with previous studies of the size distribution of atmospheric nitrate, a negative linear relationship was observed between the proportion of nitrate in the fine mode and ambient air temperature, reflecting the strong temperature dependencies of the physicochemical processes determining the gas-particle partitioning of HNO_3. However, the strength of this anticorrelation is higher when considering only the samples collected from predominantly marine air masses ($r = 0.79$) and neglecting those with back trajectories indicating influence of continental outflow [*Virkkula et al.*, 2006; *Morin et al.*, 2009].

[26] The dissimilarity observed in air mass history between the South and Central Coast regions is also reflected in the gas-phase atmospheric chemistry measurements conducted onboard R/V *Atlantis*. The mean ($\pm$ 1σ) 30 min average NO_x concentrations observed during the South and Central Coast segments of the cruise were (6.2 ± 19.8) ppbv (or nmol mol^{-1}) and (3.2 ± 9.1) ppbv, respectively, and the concentration differed between the two regions by approximately a factor of 2 during both daytime and nighttime hours (Figure 5). NO was largely absent during the night, and the molar ratio of NO_2 ($\chi NO_2 = NO_2/NO_x$) exhibited a nighttime average of 0.99 throughout the campaign, reflecting the complete titration of NO to NO_2 via oxidation by the excess ozone remaining at the end of the photochemical day. Daytime NO_2 molar ratios averaged 0.78 and 0.72 in the South and Central coast regions, respectively, and typically reached their lowest values during the period 09:00–15:00.

[27] The diurnally averaged mixing ratios of ozone and N_2O_5 for the South and Central Coast regions of the campaign are shown in Figure 6. Also shown is the diurnally averaged OH concentration, which has been calculated from spectral radiometer measurements of the photolysis rate coefficient of ozone to produce $O(^1D)$ using the parameterization developed by *Ehhalt and Rohrer* [2000]. Ozone was consistently present at higher mixing ratios in the South Coast region, averaging (40.4 ± 8.4) ppbv, while averaging (25.1 ± 8.2) ppbv in the Central Coast region. N_2O_5 reached significant concentrations only during nighttime hours (approximately 20:00–08:00), reflecting the rapid daytime loss of the NO_3 radical, which is an essential N_2O_5 precursor (Figure 1). Nighttime N_2O_5 mixing ratios averaged 11.4 and 2.3 parts per trillion by volume (pptv; or pmol mol^{-1}) for the South and Central coast regions, respectively. Collectively, the aerosol and gas-phase chemistry data reported here suggest a greater anthropogenic impact on the air masses sampled during the southern portion of the cruise [*Ryerson et al.*, 2013].

3.2. Isotopic Composition of Nitrate

3.2.1. Size-Segregated Isotopic Measurements

[28] Size-resolved measurements of the comprehensive isotopic composition of atmospheric nitrate during the R/V *Atlantis* cruise are presented in Figure 7, which shows the $\delta^{18}O$, $\Delta^{17}O$, and $\delta^{15}N$ values obtained for the coarse and fine aerosol fractions.

[29] In agreement with previous measurements of the oxygen isotopic composition of nitrate [*Hastings et al.*,

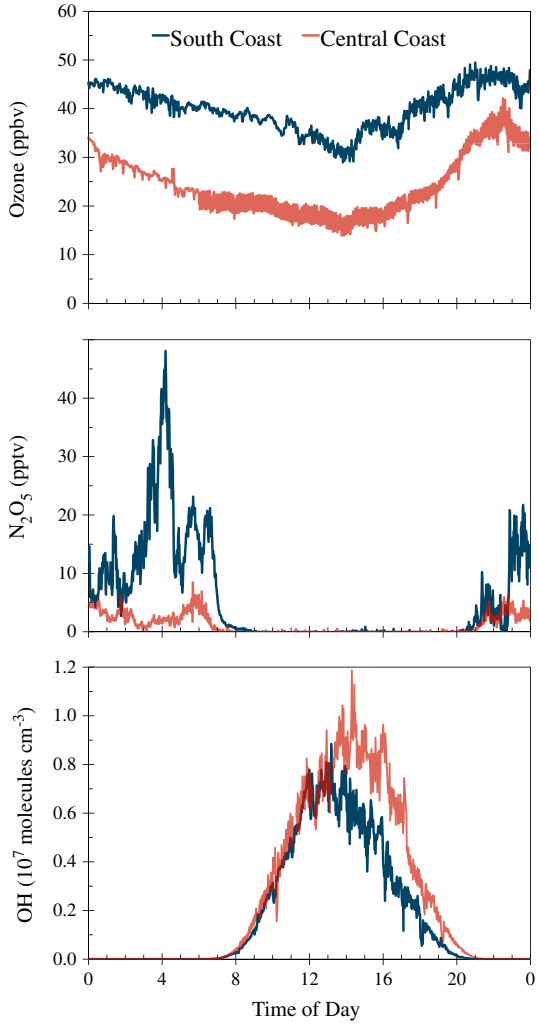

Figure 6. Diurnally averaged mixing ratios of ozone (upper) and N_2O_5 (middle) during the South and Central coast segments of the cruise. The average calculated OH concentrations are displayed in the lower panel. OH has been calculated using the parameterization developed by *Ehhalt and Rohrer* [2000], which is not strictly valid for application to the coastal MBL but should produce estimates within ± 30‰ of more sophisticated model calculations [*Sommariva et al*., 2009].

2003; *Michalski et al*., 2003; *Morin et al*., 2009], $\delta^{18}O(NO_3^-)$ was observed to vary in the range of approximately 50–90‰. When considering $\delta^{18}O(NO_3^-)$ values averaged over the duration of the campaign, no significant difference can be detected between the coarse and fine nitrate fractions ($p > 0.001$), which possessed mean values of (66.3 ± 7.6)‰ and (67.1 ± 8.3)‰, respectively. However, significant deviations (~ 20‰) in $\delta^{18}O(NO_3^-)$ between size fractions occurred for individual samples, and the average absolute difference between coarse and fine nitrate $\delta^{18}O$ was 8.0‰. Conversely, measurements of the ^{17}O-excess of nitrate, $\Delta^{17}O(NO_3^-)$, reveal significantly different patterns in the two size fractions: $\Delta^{17}O$ was systematically higher in the supermicron mode ($p < 0.001$), particularly in the South Coast region, where $\Delta^{17}O(NO_3^-)$ averaged (25.8 ± 1.7)‰ and (23.3 ± 1.8)% for the coarse and fine aerosol fractions, respectively, with an average difference of 2.6‰. This observation is consistent with the results obtained by *Morin et al*. [2009] for atmospheric nitrate in the Atlantic MBL and is also in agreement with *Patris et al*. [2007] who reported a $\Delta^{17}O(NO_3^-)$ difference of approximately 1.5‰ between the coarse and fine fractions at a coastal site in northern California (Trinidad Head) during April/May. This asymmetrical size distribution of $\Delta^{17}O(NO_3^-)$ suggests that the oxidative pathways leading to the conversion of NO_2 to nitrate are sensitive to particle size, a trend that was less pronounced in the Central Coast region, where nitrate in the supermicron and submicron fractions exhibited similar $\Delta^{17}O(NO_3^-)$ values, averaging (22.6 ± 2.2)‰ and (22.2 ± 2.0)‰, respectively ($p > 0.001$).

[30] $\delta^{15}N(NO_3^-)$ values obtained in this study are in good agreement with previous size-resolved measurements of

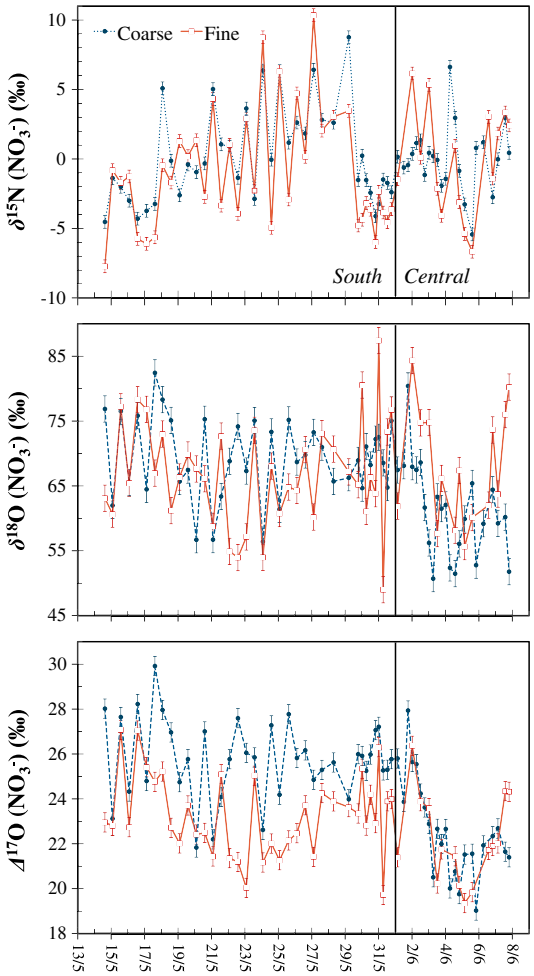

Figure 7. Time series of the comprehensive isotopic composition of atmospheric nitrate: $\delta^{15}N$ (upper panel), $\delta^{18}O$ (center panel), and $\Delta^{17}O$ (lower panel). Size-distributed coarse and fine isotopic values are represented by dashed and solid lines, respectively, with error bars representing the analytical uncertainty of the measurements (2.0‰, 0.43‰, and 0.46‰ for $\delta^{18}O$, $\Delta^{17}O$, and $\delta^{15}N$, respectively) The transit between the South and the Central Coast regions of the cruise on 1 June is indicated in each panel with a vertical black line.

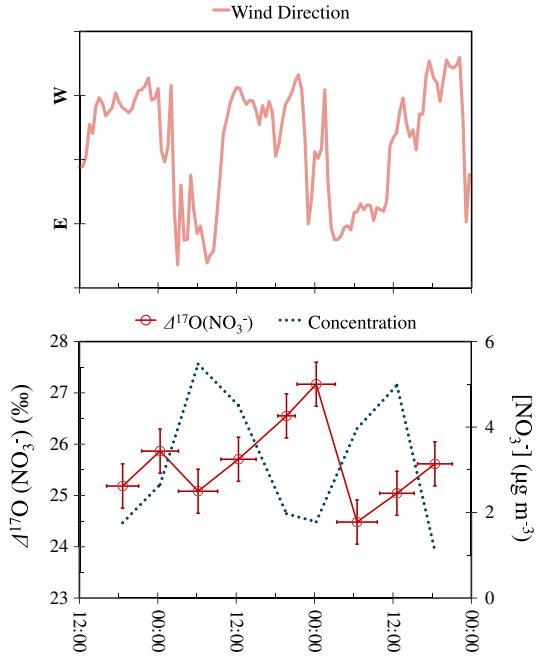

Figure 8. Bulk nitrate concentration (dotted line) and $\Delta^{17}O(NO_3^-)$ values (solid line) for the high-frequency (3–6 h) collections during 29–31 May (lower panel). The 30 min average wind direction measured onboard R/V *Atlantis* is represented by a solid line in the upper panel. Sea breeze / land breeze recirculation is inferred from the diurnal shifts between westerly (onshore) and easterly (South Coast air basin) winds.

aerosol nitrate in nonpolar regions [*Yeatman et al.*, 2001; *Morin et al.*, 2009]. Contrary to the trend observed for oxygen isotopes, no clear difference can be distinguished between the nitrogen isotope ratios of nitrate in the two aerosol size fractions ($p > 0.001$). $\delta^{15}N(NO_3^-)$ in the supermicron mode ranged between −5.4 and 8.8‰ with an average of (0.1 ± 3.1)‰, while submicron $\delta^{15}N(NO_3^-)$ values, although exhibiting a somewhat larger level of overall variability were of a comparable average value of (−0.8 ± 4.1)‰. Furthermore, the correlation between $\delta^{15}N(NO_3^-)$ in the coarse and fine aerosol modes ($r = 0.78$) was much more robust than that observed for $\Delta^{17}O$ ($r = 0.45$).

3.2.2. Bulk Isotopic Values

[31] Bulk values of $\delta^{18}O$, $\Delta^{17}O$, and $\delta^{15}N$ for atmospheric nitrate collected during each sampling period on the R/V *Atlantis* cruise have been computed by mass-weighting the values obtained for the coarse and fine aerosol fractions and have been compiled in the supporting information (Table S1) together with details regarding ship position, air mass origin, and atmospheric nitrate concentration and size distribution. The propagation of error associated with the weighting calculation results in slightly increased levels of uncertainty for the bulk isotopic values as compared to the raw size-segregated measurements (3.4‰, 0.94‰, and 0.98‰ for $\delta^{18}O$, $\Delta^{17}O$, and $\delta^{15}N$, respectively).

[32] Bulk $\Delta^{17}O(NO_3^-)$ varied in the range of 19.0 to 29.2‰ during the sampling period with an average value of (24.1 ± 2.2)‰. A clear distinction between the South and Central Coast segments of the campaign can be observed in the $\Delta^{17}O(NO_3^-)$ record: in the South Coast region, $\Delta^{17}O(NO_3^-)$ averaged (25.3 ± 1.6)‰, reaching values as high as 29‰; in contrast, samples collected from marine air masses in the Central Coast region exhibited significantly reduced ^{17}O-excess, with values decreasing markedly after the Central Coast transit (1 June) and averaging (22.3 ± 1.8)‰ during the last week of the cruise. These values are in the same general range as those previously reported for midlatitude and coastal regions [see *Alexander et al.*, 2009, and references therein], although the absolute range is somewhat larger than that previously observed. However, care should be taken in comparing our $\Delta^{17}O(NO_3^-)$ measurements to those found in the literature. Previous studies have typically employed sampling durations greater than 24 h in order to ensure the collection of an adequate amount of nitrate for isotopic analysis, a strategy that effectively masks any high-frequency variations in $\Delta^{17}O(NO_3^-)$. For example, in a 1 year study of seasonal trends in $\Delta^{17}O(NO_3^-)$ in coastal California (La Jolla), *Michalski et al.* [2003] measured values ranging from 20 to 30‰ for samples spanning several days of collection time. Similarly, in an investigation of the isotopic composition of atmospheric nitrate over a time period similar to this study, *Morin et al.* [2009] measured bulk $\Delta^{17}O(NO_3^-)$ values ranging between 24 and 33‰ for samples collected at a daily time resolution along a ship-borne latitudinal transect (approximately 28°S–52°N) in the Atlantic MBL. The detection of an equal magnitude of variability (~ 10‰) in the present study, which covered only a limited temporal and latitudinal extent (24 days and 5.8°, respectively), is thus a significant result because it indicates the presence of high-frequency variations that are superimposed on the broad temporal and spatial features of the ^{17}O-excess of nitrate. This observation can be unambiguously attributed to the strong diurnal tendency observed in the $\Delta^{17}O(NO_3^-)$ record: for the 27 samples collected on a 12 h frequency (14–27 May), $\Delta^{17}O(NO_3^-)$ averaged (24.1 ± 1.6)‰ for samples collected during the night and (26.3 ± 1.4)‰ for those collected during the day. This diurnal pattern is counterintuitive given that $\Delta^{17}O$ transfer is expected to be more significant during the night due to the instability of the NO_3 radical and absence of N_2O_5 during the day (Figure 6); however, when considering that the lifetime of nitrate against deposition is normally greater than 12 h [*Liang et al.*, 1998], this observation can be reconciled in terms of the expected ^{17}O transfer associated with daytime and nighttime reactions (i.e., atmospheric nitrate collected during the night is likely to have been produced from NO_x oxidation occurring during the preceding day and vice versa). This impact of lifetime on $\Delta^{17}O(NO_3^-)$ dynamics has been recently observed at a coastal site in the UK [*Bateman and Kaiser*, 2010] and has also been predicted by numerical modeling studies that account for the diurnality of nitrate production [*Morin et al.*, 2011]; however, the present report represents, to the best of our knowledge, the first detailed observational account of diurnal variations in the $\Delta^{17}O$ of nitrate.

[33] The phase shift between the $\Delta^{17}O$ of nitrate and its precursor molecules was likely reinforced and magnified in the present study due to a persistent diurnal sea breeze / land breeze recirculation in the South Coast air basin, which has been inferred from Doppler wind profile measurements at Los Angeles International Airport as described by *Wagner*

et al. [2012]. This thermally induced recirculation is a well-known mesoscale phenomenon in which a strong daytime sea breeze brings marine air into the Los Angeles basin, driving polluted urban air masses eastward [*Gentner et al*., 2009], while a weaker land breeze transports urban emissions and their accumulated secondary species out of the basin and over Santa Monica Bay during the night [*Cass and Shair*, 1984]. Air masses residing over the California coast during the day are likely to be impacted by a return flow aloft that contains emissions from the nighttime or late in the preceding day [*Lu and Turco*, 1994, 1995]. The impact of this recirculation on the temporal evolution of nitrate concentration and $\Delta^{17}O$ is most evident for the period 29–31 May, when nine consecutive samples were collected at relatively short sampling frequencies (3–6 h) under sea breeze / land breeze transitions in Santa Monica Bay. From inspection of Figure 8, it is clear that $\Delta^{17}O(NO_3^-)$ was associated with the wind direction measured onboard R/V *Atlantis* during this period with values decreasing during the land breeze phase (easterly wind) of recirculation, which typically began at midnight and continued until approximately 06:00, and increasing during the sea breeze phase (westerly wind), reaching maximum daily values at midnight. The atmospheric concentration of nitrate exhibited an opposite trend with respect to wind direction during this time, reaching maximum values (~ 4–5 $\mu g\,m^{-3}$) during the nocturnal land breeze and decreasing rapidly upon the transition to westerly marine flow. This observation suggests that the land breeze was likely dominated by nitrate produced through OH channel (R8) that had accumulated within the Los Angeles Basin during the day, while samples collected from the sea breeze were composed mostly of nitrate that had been produced through nocturnal reactions ((R11)–(R13)) over water and returned to the coastal sampling location with the sea breeze in the morning.

[34] Bulk aerosol $\delta^{15}N(NO_3^-)$ values ranged between −6.2 and 8.0‰ during the campaign with an average value of (0.0 ± 3.2)‰. This mean and range of values is typical for $\delta^{15}N(NO_3^-)$ measurements in extrapolar regions [*Freyer*, 1991; *Yeatman et al*., 2001; *Hastings et al*., 2003; *Baker et al*., 2007; *Morin et al*., 2009]; however, in disagreement with some of these studies, where large ^{15}N enrichments have been observed for nitrate of anthropogenic origin, there is no apparent correlation between $\delta^{15}N(NO_3^-)$ and air mass origin in the present study. For example, despite the significant differences in back trajectories and atmospheric nitrate concentration (Figure 4) observed in the two major sampling regions, no systematic difference can be detected in the nitrogen isotopic composition of nitrate collected during the South and Central Coast cruise legs, where $\delta^{15}N(NO_3^-)$ averaged (0.0 ± 3.5)‰ and (0.0 ± 2.6)‰, respectively ($p > 0.001$); although, when considering the mass-weighted 24 h averages, a small difference can be detected (averages of 0.8‰ for the South Coast and −0.1‰ for the Central Coast).

[35] A particularly remarkable feature of the $\delta^{15}N(NO_3^-)$ record is the diurnal pattern observed, which is suggestive of isotopic effects associated with either the photolytic cycling of NO_2 or the conversion of NO_2 to nitrate. This is a significant result considering the long standing debate over the relative importance of NO_x sources, ^{15}N partitioning within the NO_x cycle, and the effect of atmospheric transport in determining temporal variations in the $\delta^{15}N$ of atmospheric nitrate [*Hastings et al*., 2003; *Jarvis et al*., 2008; *Morin et al*., 2008; *Morin et al.*, 2009]. For the 27 diurnal samples (14–27 May), $\delta^{15}N(NO_3^-)$ averaged (2.1 ± 3.9)‰ for nighttime collections and (−1.2 ± 2.2)‰ for samples collected during the day. Considering the temporal offset between NO_x cycling and nitrate production suggested by the $\Delta^{17}O(NO_3^-)$ record, this observation indicates that increased ^{15}N values are associated with daytime nitrate production (i.e., OH channel). Similar to the case with $\Delta^{17}O(NO_3^-)$, this is the first study to report direct observational evidence of diurnal variations in atmospheric $\delta^{15}N(NO_3^-)$.

4. Discussion

4.1. Interpretation of $\Delta^{17}O(NO_3^-)$ Measurements

[36] The general mass balance equation (also termed the "continuity equation") governing the temporal evolution of the concentration of nitrate in a given air parcel is given by

$$\frac{d}{dt}\left[NO_3^-\right] = \sum_i P_i - L \tag{2}$$

where the atmospheric concentration of nitrate, denoted $[NO_3^-]$, is expressed in cm^{-3}. P_i and L represent the individual source rates and total sink rate of NO_3^- (in $cm^{-3}\,s^{-1}$), respectively, which include both chemical reactions within the parcel and fluxes at its boundaries.

[37] The implementation of $\Delta^{17}O$ into the mass balance equation follows from the conservation of mass applied to the ^{17}O-excess. The key assumption behind this approach is that sink reactions do not induce a specific non-mass-dependent fractionation and that every source reaction induces the transfer of a given $\Delta^{17}O$ value to the nitrate produced. This assumption would not be applicable to isotopic enrichment (δ) values or fractionation effects would have to be taken into account for every reaction considered. Therefore, while $\delta^{18}O(NO_3^-)$ results have been provided in the auxiliary materials (Table S1) for comparison to previous studies and to allow for the computation of $\delta^{17}O(NO_3^-)$, they are not discussed in the following analysis.

[38] The continuity equation for $\Delta^{17}O(NO_3^-)$ can be stated as follows:

$$\frac{d}{dt}\left(\left[NO_3^-\right] \times \Delta^{17}O\left(NO_3^-\right)\right) = \sum_i \left(P_i \times \Delta^{17}O\left(NO_3^-\right)_i\right) - \left(L \times \Delta^{17}O\left(NO_3^-\right)\right) \tag{3}$$

where $\Delta^{17}O(NO_3^-)_i$ is the specific $\Delta^{17}O$ signature induced by the nitrate production channel P_i ((R8), (R10), (R11), and (R13)) [*Morin et al*., 2011]. In practice, $\Delta^{17}O(NO_3^-)_i$ values are estimated as a function of the $\Delta^{17}O$ of the precursors involved in a given nitrate production channel using mass balance calculations that trace the origin of oxygen atoms transferred during the chemical transformation of NO_x in the atmosphere. This approach, which springs from the pioneering work of *Lyons* [2001] and *Michalski et al*. [2003], has been applied in several studies to assess seasonal variations in NO_x transformation processes at regional to global scales [*Alexander et al*., 2004, 2009; *Michalski et al*., 2005; *McCabe et al*., 2007; *Morin et al*., 2007, 2008, 2009, 2012; *Patris et al*., 2007; *Savarino et al*., 2007, 2013; *Kunasek et al*., 2008]. In this study, we have estimated

$\Delta^{17}O(NO_3^-)_i$ values for the nitrate production reactions previously discussed using the diurnally integrated isotopic signature (DIIS) values modeled by *Morin et al*. [2011] for 45° N. DIIS values implicitly integrate seasonal variations in the $\Delta^{17}O$ of NO_2 that occur due to changes in the activity of ozone (R3) relative to the peroxy radicals ((R4)/(R5)), which are derived from O_2 and possess negligible ^{17}O-excess [*Savarino and Thiemens*, 1999]. Estimates of $\Delta^{17}O(NO_3^-)_i$ are highly sensitive to the value used for $\Delta^{17}O(O_3^*)$, which is the $\Delta^{17}O$ value of ozone that is transferred during bimolecular reactions in the troposphere [*Morin et al*., 2011]. We have scaled the DIIS functions to a $\Delta^{17}O(O_3^*)$ of 41‰, an average of measurements in the Atlantic MBL during a cruise in the spring of 2012 [*Savarino et al*., 2013], obtained using a recently developed analytical technique with an uncertainty of ± 3‰ [*Vicars et al*., 2012]. This value is consistent in terms of $\Delta^{17}O(O_3)_{bulk}$ with the average of existing measurements of ozone isotopic composition obtained using the traditional "cryogenic technique" [*Johnston and Thiemens*, 1997; *Krankowsky et al*., 1995]; furthermore, this value is only slightly higher than that used in the landmark study of atmospheric nitrate isotopes by *Michalski et al*. [2003] who adopted an effective $\Delta^{17}O(O_3^*)$ value of 35‰ [*Morin et al*., 2007]. By adopting a $\Delta^{17}O(O_3^*)$ value of 41‰, we have calculated the $\Delta^{17}O$ signatures of the (R8), (R11), and (R13) nitrate production pathways (see section 1) to be 18.6‰, 36.6‰, and 30.2‰, respectively.

[39] Solving numerically the system of equations formed by equations (2) and (3) simultaneously yields the time evolution of the concentration and $\Delta^{17}O$ of atmospheric nitrate. By decomposing the left-hand side of equation (3) and reorganizing, we obtain

$$\left[NO_3^-\right] \times \frac{d}{dt}\left(\Delta^{17}O\left(NO_3^-\right)\right) = \sum_i \left(P_i \times \Delta^{17}O\left(NO_3^-\right)_i\right) - \Delta^{17}O\left(NO_3^-\right) \times \left(L \times \frac{d}{dt}\left[NO_3^-\right]\right) \quad (4)$$

[40] Substituting the last term using equation (2), we have

$$\left[NO_3^-\right] \times \frac{d}{dt}\left(\Delta^{17}O\left(NO_3^-\right)\right) = \sum_i \left(P_i \times \Delta^{17}O\left(NO_3^-\right)_i\right) - \Delta^{17}O\left(NO_3^-\right) \times \sum_i P_i \quad (5)$$

[41] After a final organization, we obtain

$$\frac{d}{dt}\left(\Delta^{17}O\left(NO_3^-\right)\right) = \sum_i \frac{P_i}{\left[NO_3^-\right]} \times \left(\Delta^{17}O\left(NO_3^-\right)_i - \Delta^{17}O\left(NO_3^-\right)\right) \quad (6)$$

[42] In plain words, we find that the time derivative of $\Delta^{17}O(NO_3^-)$ should scale as the sum of nitrate production rates multiplied by the deviation of their isotopic signature to the current $\Delta^{17}O$ value. Equation (6) can be further modified by introducing P_{total}, the total nitrate production rate:

$$\frac{d}{dt}\left(\Delta^{17}O\left(NO_3^-\right)\right) = \frac{P_{total}}{\left[NO_3^-\right]} \times \sum_i \frac{P_i}{[P_{total}]} \times \left(\Delta^{17}O\left(NO_3^-\right)_i - \Delta^{17}O\left(NO_3^-\right)\right) \quad (7)$$

[43] Note that

$$\frac{P_{total}}{\left[NO_3^-\right]} = \frac{1}{\tau} \quad (8)$$

where τ is the atmospheric lifetime of nitrate.

[44] Equation (7) thus provides a general mathematical formalism to evaluate temporal variations in $\Delta^{17}O(NO_3^-)$ in terms of the relative proportions of the production channels and atmospheric lifetime of nitrate. Until now, quantitative interpretations of $\Delta^{17}O(NO_3^-)$ measurements have been dependent on the implicit assumption of isotopic steady state. This assumption is equivalent to setting the left-hand side of equation (7) to zero (i.e., hypothesized static $\Delta^{17}O(NO_3^-)$ time derivative), which results in the steady state formalism introduced by *Michalski et al*. [2003]:

$$\Delta^{17}O\left(NO_3^-\right) = \sum_i \frac{P_i}{P_{total}} \times \left(\Delta^{17}O\left(NO_3^-\right)_i\right) \quad (9)$$

[45] The steady state approach has proven useful in the interpretation of seasonal-scale dynamics using $\Delta^{17}O(NO_3^-)$ observations averaged over several days; however, equation (9) does not adequately address variations at temporal scales smaller than the atmospheric lifetime of nitrate (e.g., diurnal variations). In the case of high-frequency $\Delta^{17}O(NO_3^-)$ observations, the physical loss of nitrate through deposition must be explicitly taken into account using equation (7). In the analysis that follows, we will utilize both approaches in their appropriate contexts. First, $\Delta^{17}O(NO_3^-)$ measurements aggregated over 48 h periods (i.e., a time period greater than or equal to the lifetime of nitrate, as is shown in section 4.1.2) will be interpreted using the traditional steady state formalism, which allows for a semiquantitative assessment of the differences in nitrate formation pathways between the South and Central Coast segments of the cruise (section 4.1.1). The steady state assumption will then be relaxed, and the general mass balance equation will be applied in a detailed analysis of the diurnal variations observed during the period 14–27 May (section 4.1.2).

4.1.1. Steady State Evaluation of $\Delta^{17}O(NO_3^-)$

[46] If the average contributions from at least two of the (R8), (R10), (R11), or (R13) pathways are known or can be neglected, the relative contributions from the remaining two pathways can be derived using the steady state mass balance equation (equation (9)). The impact of halogen-mediated nitrate production from the heterogeneous XNO_3 pathway (R10) is difficult to assess in the present study due to the absence of XO or XNO_3 measurements during the cruise on R/V *Atlantis*. However, while this pathway can be quite significant in some environmental contexts [*Morin et al*., 2007; *Savarino et al*., 2013], chemistry-involving reactive halogen species is generally not expected to account for a considerable fraction of nitrate production in midlatitude regions impacted by anthropogenic NO_x emissions [*Sander et al*., 1999; *Parrella et al*., 2012]. Therefore, we will neglect for now the (R10) channel and consider only the (R8), (R11), and (R13) pathways. Of these three major nitrate formation channels, direct H abstraction by the NO_3 radical via reaction with DMS (R11), which was the dominant reaction of the type NO_3 + RH during the cruise on R/V *Atlantis* [*Wagner*

Table 1. Mass-Weighted 48 h Averages of $\Delta^{17}O(NO_3^-)$ for the Coarse, Fine, and Bulk (Weighted) Aerosol Fractions[a]

Collection Dates	$\Delta^{17}O(NO_3^-)$ (‰)			P_{R13}/P_{total} (%)		
	Bulk	Coarse	Fine	Bulk	Coarse	Fine
14–15 May	24.6	24.6	24.4	40	40	39
16–17 May	27.1	27.4	25.9	62	64	51
18–19 May	23.4	23.5	23.0	30	31	26
20–21 May	24.1	24.3	22.8	36	38	24
22–23 May	24.5	25.0	21.3	39	43	12
24–25 May	25.8	26.3	22.0	50	55	17
26–28 May	24.7	25.4	23.2	41	47	28
29–30 May	24.8	25.0	23.7	42	43	32
31 May–1 June	25.0	25.8	22.4	44	50	21
2–3 June	23.9	24.3	22.0	34	38	17
4–5 June	20.7	20.9	20.5	6	9	4
6–7 June	22.2	22.1	22.5	19	18	22

[a]The estimated relative production from the nocturnal N_2O_5 pathway has been calculated using the steady state approximation of equation (9), assuming that $\Delta^{17}O(O_3^*) = 41‰$ and the relative importance of the NO_3-DMS pathway to nitrate production averages 7.5%.

et al., 2012], is thought to play the least significant role in nitrate production. For example, using a global aerosol-oxidant model, *Alexander et al*. [2009] obtained an average annual contribution from the (R11) pathway equal to only 4% of total nitrate production and *Michalski et al*. [2003] modeled a contribution from this pathway that varied between 1 and 10% on an annual basis at La Jolla, California. If P_{R11}/P_{total} is assumed to account for a (7.5 ± 5)% of total nitrate production during this study, the same range adopted by *Patris et al*. [2007], equation (9) can be rearranged and solved for the fractional contribution of the nocturnal N_2O_5 pathway (P_{R13}/P_{total}) by using 48 h averages of $\Delta^{17}O(NO_3^-)$ as input. The results of this computation for the coarse, fine, and bulk (weighted) aerosol fractions are presented in Table 1.

[47] Mass-weighting the subdiurnal isotopic measurements over 48 h periods eliminates much of the temporal variability observed in the time series and reveals an average $\Delta^{17}O(NO_3^-)$ of ~ 25‰ for the South Coast region, a seasonal signature for coastal California that is consistent with previous measurements and modeling studies [*Michalski et al*., 2003; *Alexander et al*., 2009]. Individual 48 h averages generate estimates of relative nitrate production via the N_2O_5 pathway (P_{R13}/P_{total}) that vary between 30 and 62%, with an average of (42 ± 10)%, suggesting that this pathway played a quantitatively significant and sometimes dominant role in terms of NO_x removal in the air masses sampled in this region. This finding is consistent with recent studies that have found nocturnal processes to have a significant impact on the reactive nitrogen budget, converting a comparable amount of NO_x as daytime reactions in air masses impacted by anthropogenic emissions [*Brown et al*., 2004, 2006]; furthermore, the range of inferred P_{R13}/P_{total} values obtained here is in excellent quantitative agreement with estimates for La Jolla during May/June (~ 30–50%) based on atmospheric box modeling by *Michalski et al*. [2003]. *Patris et al*. [2007] derived somewhat higher contributions from the (R13) pathway (~ 50–80%) from $\Delta^{17}O(NO_3^-)$ measurements in the MBL at Trinidad Head, California, during April/May, although we suspect that the significance of the (R13) pathway was likely overestimated in this study due to the use of a low $\Delta^{17}O$ signature for N_2O_5 hydrolysis in the mass balance calculations (25.7‰).

[48] The largest relative contributions from the N_2O_5 channel are attributed to the period 16–17 May, when the R/V *Atlantis* was stationed overnight in the Santa Monica Bay and sustained sea breeze / land breeze recirculation resulted in nitrate concentration maxima in both the coarse and fine modes (Figure 3). Daytime (sea breeze) nitrate collections during this period exhibited considerably elevated $\Delta^{17}O(NO_3^-)$ values (> 27‰), corresponding to a 48 h average P_{R13}/P_{total} estimate of 62%. Subsequent peaks in nocturnal nitrate production occurred when the R/V *Atlantis* had returned to Santa Monica Bay (20–21, 24–25, 29–31 May) and are also associated with periods of persistent nighttime outflow from the Los Angeles metropolitan region [*Wagner et al*., 2012]. Conversely, periods of predominantly onshore atmospheric transport (e.g., 18–19, 22–23, and 26–28 May) correspond to relatively low atmospheric nitrate concentrations and reduced contributions from the (R13) channel. Similarly, the low 48 h average $\Delta^{17}O(NO_3^-)$ values obtained for samples collected in the Central Coast region (1–7 June) correspond to estimates of contributions from the N_2O_5 pathway that vary between 6 and 34%, indicating that the daytime $OH + NO_2$ channel was the dominant NO_x sink in the marine air masses sampled in this region (60–85%). The observation of significant contributions from N_2O_5 hydrolysis in polluted air masses from continental outflow, as well as the broad differences in $\Delta^{17}O(NO_3^-)$ and air mass origin detected between the two main sampling regions, suggests a strong spatial coupling of anthropogenic emissions and nighttime chemistry [*Andreae and Crutzen*, 1997].

[49] Due to the relatively long lifetimes of gaseous HNO_3 and particulate nitrate (several hours and several days, respectively) [*Liang et al*., 1998; *Brown et al*., 2004; *Millet et al*., 2004], the in situ atmospheric chemistry data obtained during the cruise on R/V *Atlantis* is not directly reflective of the nitrate collected during any individual sampling period. For example, it appears that nitrate concentration gradients during periods of sea breeze / land breeze recirculation were determined primarily by source variability and mixing rather than in situ chemical production. In this case, a robust evaluation of nitrate isotope measurements in terms of parallel atmospheric measurements would require the use of a chemical transport model (CTM) to predict the evolution of nitrate along the trajectories of the air masses sampled, a modeling effort that is beyond the scope of this study. However, the general trends observed in precursor gas concentrations are broadly indicative of the differences in daytime and nighttime NO_x processing between the two main sampling regions. The average nighttime N_2O_5 mixing ratio in the Central Coast (2.3 pptv) was significantly lower than that observed during the southern section of the cruise (11.4 pptv) and also much lower than previous observations of N_2O_5 in the MBL reported in the literature [*Brown et al*., 2004; *Sommariva et al*., 2009; *McLaren et al*., 2010]. N_2O_5 concentrations were typically below the limit of detection (~1 pptv) during the period 4–5 June, when $\Delta^{17}O(NO_3^-)$ reached its lowest values and the inferred contributions from the heterogeneous pathway amount to 6%. On the other hand, because the NO_2 and parameterized OH concentrations were similar throughout the study (Figures 5 and 6, respectively), any differences between the two regions in the rate

of HNO_3 production from the $OH + NO_2$ reaction can be assumed to be disproportionately small compared to the differences in N_2O_5 concentration. In other words, it seems reasonable to assume that the relative importance of the N_2O_5 hydrolysis pathway was greater in the South Coast, simply based on a consideration of the precursor measurements. Therefore, the broad spatial variability in the relative importance of nocturnal NO_x processing inferred from the South and Central Coast $\Delta^{17}O(NO_3^-)$ records seem to be largely supported by the in situ atmospheric chemistry data obtained during the cruise on R/V *Atlantis*.

[50] The systematically elevated $\Delta^{17}O(NO_3^-)$ observed in the supermicron aerosol fraction in the South Coast region amounts to a large difference in terms of the resulting nitrate budget calculations (Table 1): on average, 49% of nitrate in the coarse mode is attributed to the N_2O_5 pathway in this region as compared to 32% in the submicron mode. This observation is consistent with all previous size-distributed measurements of the $\Delta^{17}O$ of atmospheric nitrate in the MBL [*Patris et al*., 2007; *Morin et al*., 2009] and suggests that the size distribution of $\Delta^{17}O$ is determined largely by the physical characteristics of the individual precursor gases (HNO_3, NO_3, N_2O_5, etc.), with heterogeneous N_2O_5 reactions occurring preferentially on the surface of supermicron particles. This greater relative importance of the coarse aerosol fraction as a sink for N_2O_5 in coastal and marine regions may indicate an increased efficiency of N_2O_5 hydrolysis on deliquesced sea-salt particles, which represent a large fraction of total aerosol surface area in the MBL. Indeed, measurements of aerosol size distribution (see supporting information Figure S1) indicate that surface area concentrations were frequently elevated ($> 100\,\mu m^2\,cm^{-3}$) in the supermicron mode during the South Coast section of the cruise. However, the surface area concentrations observed in the supermicron mode were not typically higher than those observed in the submicron mode; therefore, the higher $\Delta^{17}O(NO_3^-)$ values observed in the coarse fraction during the South Coast section of the cruise cannot be explained by aerosol physical properties alone. Alternatively, increased $\Delta^{17}O(NO_3^-)$ values in the coarse fraction could also result from the reaction between N_2O_5 and particulate chloride (Cl^-) (R14), which is abundant in coarse marine aerosol. Reactive chlorine measurements during the R/V *Atlantis* cruise suggest that the (R14) pathway represented a significant N_2O_5 loss mechanism in the South Coast region, particularly during nights spent in Santa Monica Bay (e.g., 16, 21, 24, and 25 May) when $ClNO_2$ concentrations greater than 500 pptv were observed during the land breeze circulation phase between approximately 03:00 and 06:00 [*Riedel et al*., 2012; *Wagner et al*., 2012]. Coarse fraction $\Delta^{17}O(NO_3^-)$ values were greater than 27‰ for samples collected on the days following these high nighttime $ClNO_2$ events; furthermore, coarse $\Delta^{17}O(NO_3^-)$ was enriched 4–6‰ over the fine fraction for these samples. *Hayes et al*. [2013] note that sea-salt aerosol measured in the Los Angeles Basin was substantially depleted in Cl^- during the cruise on R/V *Atlantis*, presumably due to nocturnal atmospheric processing involving reactive uptake of N_2O_5; they further noted a parallel increase in supermicron aerosol nitrate, consistent with our findings. Based on these observations, we tentatively suggest that the association of higher $\Delta^{17}O(NO_3^-)$ values with coarse aerosol observed in this study and others results from an enhanced importance of the (R14) pathway in the MBL; furthermore, our results suggest that high frequency size-distributed $\Delta^{17}O(NO_3^-)$ measurements could be a useful tool for evaluating the magnitude and spatiotemporal variability of this sink, a potential application of nitrate stable isotopes that is deserving of further study.

[51] $\Delta^{17}O(NO_3^-)$ did not vary widely with particle size for samples collected in the Central Coast region (Figure 7), corresponding to estimates of contributions from the (R13) pathway of 22% and 15% for coarse and fine particles, respectively. This observation is similar to that of *Patris et al*. [2007], who reported comparable contributions from the N_2O_5 pathway for coarse and fine aerosol in air masses transported to the California coast from Asia and attributed this observation to the redistribution of nitrate during long-range transport. The difference in air mass origin and $\Delta^{17}O(NO_3^-)$ observed between the South and Central Coast regions offers a potential explanation for these observations: atmospheric residence time declines sharply as a function of diameter for particles $> 1\,\mu m$, while fine particle nitrate exhibits a lower deposition velocity and remains suspended in the atmosphere for longer periods [*Chen et al*., 2007]. Atmospheric deposition during long-range transport may thus result in the disproportionate removal of nitrate produced through the N_2O_5 pathway when it accumulates preferentially in the coarse fraction (e.g., due to the (R14) pathway). Therefore, the observation of a constant size distribution for both mass (Figure 3) and $\Delta^{17}O(NO_3^-)$ (Figure 7) in the Central Coast can be interpreted as further evidence that the nitrate sampled in this region was likely transported long distances across the ocean, providing a background source of nitrate with a low $\Delta^{17}O(NO_3^-)$ value that disrupted the variability induced by emissions from the continent.

[52] It should be recognized that the estimates of P_{R13}/P_{total} shown in Table 1 are only semiquantitative due to potential biases resulting from the assumptions drawn regarding the isotopic composition of ozone ($\Delta^{17}O(O_3^*) = 41‰$) and the relative proportions of nitrate production from the halogen ($P_{R10}/P_{total} = 0\%$) and DMS ($P_{R11}/P_{total} = 7.5\%$) channels. Variations in the (R10) and (R11) pathways introduce modest uncertainties. For example, variability in the DMS pathway induces an error of ± 8% in terms of the resulting estimate of P_{R13}/P_{total} when P_{R11}/P_{total} is allowed to fluctuate in the range of 2.5–12.5% (i.e., ± 5%). Furthermore, we estimate a relatively small 6–12% decrease in P_{R13}/P_{total} when 5–10% of total nitrate production is attributed to the daytime halogen pathway in equation (9), assuming an isotope transfer similar to that proposed for $BrNO_3$ hydrolysis by *Morin et al*. [2009]. However, quantitative estimates of contributions from the N_2O_5 pathway are exceptionally sensitive to the $\Delta^{17}O(O_3^*)$ value chosen in the calculation: for example, allowing $\Delta^{17}O(O_3^*)$ to vary by ± 3‰ (the analytical uncertainty of the method used for ozone isotope analysis) results in a recalculation of P_{R13}/P_{total} on the order of ± 15%. If we consider a relatively large 34–48‰ range of potential $\Delta^{17}O(O_3^*)$ values, the higher end of the 25–48‰ range evaluated in a global model by *Alexander et al*. [2009], the resulting average P_{R13}/P_{total} estimate for the South Coast region varies between 7 and 82%, thus inverting the potential atmospheric interpretation resulting from the same $\Delta^{17}O(NO_3^-)$ value. Clearly, the quantification

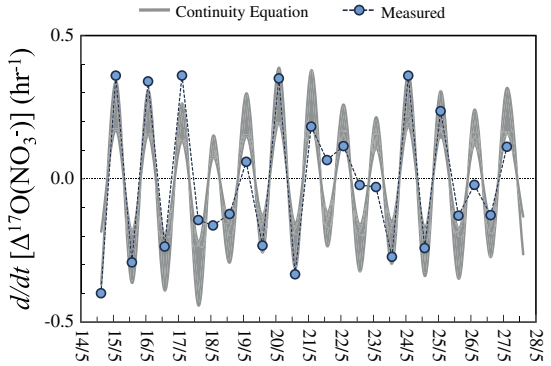

Figure 9. Comparison of the $\Delta^{17}O(NO_3^-)$ derivatives observed in this study with those generated by constraining the continuity equation to our measurements at τ values of 24 and 48 h. The spread between these two cases is represented as a grey shaded region.

of the nitrate production budget from $\Delta^{17}O(NO_3^-)$ is highly dependent on the value of $\Delta^{17}O(O_3^*)$ adopted in the mass balance calculation, which underscores the need for further field measurements to better constrain the ^{17}O-excess of ozone [*Morin et al*., 2007; *Vicars et al*., 2012]. In the next section, we will demonstrate how the diurnal variations observed for $\Delta^{17}O(NO_3^-)$ in this study can be used to eliminate unrealistic assumptions regarding the value used for $\Delta^{17}O(O_3^*)$.

4.1.2. Diurnal Variations in $\Delta^{17}O(NO_3^-)$

[53] One of the most remarkable features of the $\Delta^{17}O(NO_3^-)$ record obtained for the cruise on R/V *Atlantis* is the pronounced diurnal variability observed during the period 14–27 May, when samples were collected at a 12 h frequency allowing for direct daytime/nighttime comparisons. These diurnal cycles indicate that the lifetime of atmospheric nitrate is sufficiently short in some cases that $\Delta^{17}O(NO_3^-)$ reflects variations in the relative contributions of daytime and nighttime oxidation pathways. Such variations cannot be interpreted within the traditional steady state framework used in the previous section; however, the general mass balance equation (continuity equation) repeated below can be used to evaluate these diurnal fluctuations in $\Delta^{17}O(NO_3^-)$ by accounting for nitrate sinks (i.e., the atmospheric lifetime of nitrate against wet and dry deposition):

$$\frac{\mathrm{d}}{\mathrm{d}t}\left(\Delta^{17}\mathrm{O}\left(\mathrm{NO_3^-}\right)\right) = \frac{1}{\tau} \times \sum_i \frac{P_i}{[P_{\mathrm{total}}]} \times \left(\Delta^{17}\mathrm{O}\left(\mathrm{NO_3^-}\right)_i - \Delta^{17}\mathrm{O}\left(\mathrm{NO_3^-}\right)\right) \quad (10)$$

[54] In the following analysis, we will consider the same three nitrate production pathways discussed in Section 4.1.1, namely, the (R8), (R11), and (R13) channels, and apply the same assumptions regarding $\Delta^{17}O(O_3^*)$ and P_{R10}/P_{total}. The rate of the (R8) reaction is negligible during the night due to the rapid loss of the OH radical after 20:00 (Figure 6) and can therefore be considered only during daytime hours (08:00–20:00). Due to the instability of the NO_3 radical during the day, the rate of nitrate production through the (R11) and (R13) channels can be considered only for nighttime hours (20:00–08:00). It is possible that the lifetime of the NO_3 radical against photolysis can be sufficiently long in some cases to lead to the daytime production of HNO_3 [*Brown et al*., 2005]; however, the assumption of a negligible daytime contribution from this pathway seems to be substantiated by the in situ measurements of N_2O_5 (Figure 6), which was found to be largely absent during the day. Because the (R8) and (R11)/(R13) production channels are restricted to daytime and nighttime hours, respectively, the values of P_i/P_{total} can be assumed a priori in the case of samples collected on a diurnal frequency (collections periods were approximately 08:00–19:00 and 19:00–08:00 for daytime and nighttime collections, respectively). This greatly simplifies the mass balance calculation and allows for an evaluation of the temporal evolution of $\Delta^{17}O(NO_3^-)$ solely in terms of the atmospheric lifetime of nitrate.

[55] The lifetime of nitrate in the troposphere can vary widely and it cannot be calculated directly from the gas-phase measurements made onboard. Given that τ is typically greater than 12 h for gaseous HNO_3 and particulate nitrate [*Liang et al*., 1998; *Millet et al*., 2004], each HVAS sample can be expected to reflect both daytime and nighttime nitrate production, not exclusively one or the other. Variability in the lifetime of nitrate sampled during the cruise can be expected to result in a disagreement between the observed changes in $\Delta^{17}O(NO_3^-)$ and those calculated using equation (10) with a constant value of τ. If we consider the range of results calculated using τ values between 24 and 48 h and ignore for now any potential variability outside of this range, we can compare the time derivative of $\Delta^{17}O(NO_3^-)$ observed in this study with that predicted by the continuity equation as shown in Figure 9. Linear regression analysis reveals a significant correlation between these two variables ($r = 0.84$, $n = 27$), indicating that the continuity equation accurately describes the general trend observed in the data; furthermore, the absolute magnitude of the observed variability is in good agreement with that computed by constraining the continuity equation to our $\Delta^{17}O(NO_3^-)$ measurements, suggesting that the adopted range value of τ values (24–48 h) is appropriate in many cases. The calculated values are more consistent with the observations during periods of sustained sea breeze / land breeze recirculation in the Los Angeles Basin, such as during the period 14–17 May, when both the concentration and $\Delta^{17}O$ of nitrate reached maximum values; conversely, periods of predominantly onshore flow (e.g., 18–19 May, 23 May, 26–27 May) seem to cause a disruption in the temporal evolution of $\Delta^{17}O(NO_3^-)$, presumably by delivering nitrate from the remote MBL to the coastal sampling location and displacing continental air masses laden with anthropogenic nitrate, an assertion that is consistent with the decreased atmospheric concentrations observed during these periods (Figure 3). Because the magnitudes of the observed variations in $\Delta^{17}O(NO_3^-)$ are much smaller than that predicted by the continuity equation during periods of marine transport, it seems likely that the nitrate sampled at these times possessed a longer atmospheric lifetime, thus partially masking the extent of diurnal variability, consistent with the arguments developed in section 4.1.1 regarding the size distribution of nitrate and atmospheric lifetime.

[56] By using the measured $\Delta^{17}O(NO_3^-)$ values as input, we have quantified the atmospheric lifetime of the nitrate sampled during the period 14–27 May by rearranging equation (10) and solving directly for τ. The results of this computation are shown in Figure 10 along with the total

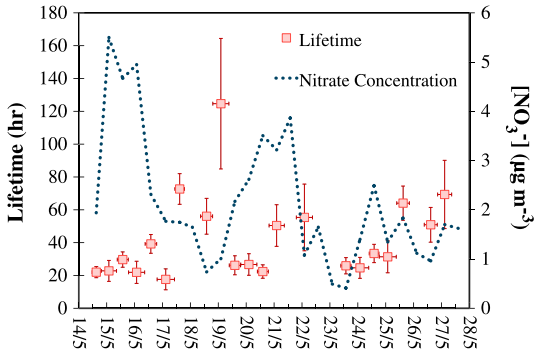

Figure 10. Time series showing variations in the lifetime of atmospheric nitrate (squares) as calculated using equation (10) for the period 14–27 May. The error bars represent the uncertainty induced by allowing $\Delta^{17}O(O_3^*)$ to vary by ± 3‰ in the continuity equation calculation. The total atmospheric nitrate concentration (secondary *y* axis) is represented by a dotted line.

atmospheric nitrate concentration. It should be borne in mind that our estimates of τ likely represent "apparent" lifetimes as the continuity equation produces unreliable results during episodes of instability in air mass origin as the underlying assumption of following a given air parcel is violated. For example, changes in $\Delta^{17}O$ that are in the opposite direction than predicted by the continuity equation result in negative τ values for five samples (data not shown in Figure 10) and occur in conjunction with transitions from continental to marine atmospheric transport in all cases. However, the τ values obtained for the majority of samples are in good agreement with those typically encountered in the literature. For example, *Liang et al*. [1998] used a photochemical model to simulate NO_x cycling in the industrialized eastern U.S. and obtained average τ values for nitrate ranging from 12 h in the spring to 26 h in the fall. The τ values estimated in this study, which vary within the range of 18 to 39 h during periods of nighttime continental outflow to the Santa Monica Bay [*Wagner et al*., 2012], are largely consistent with these findings. Furthermore, these values substantiate the assumption made in section 4.1.1 regarding the lifetime of nitrate (i.e., $12\,h < \tau < 48\,h$). Estimates of τ are higher for samples collected during periods of marine transport, typically ranging from 2 to 3 days and reaching values as high as 5 days. *Millet et al*. [2004] used a variability-lifetime approach to estimate the lifetime of submicron particulate nitrate in air masses arriving at the California coast (Trinidad Head) from the Pacific Ocean and obtained average values of 3 to 7 days, consistent with our estimates for onshore flow periods. Assuming a boundary layer depth of 900 m over the California coast [*Wood and Bretherton*, 2004], the atmospheric lifetimes inferred in this study correlate to deposition velocities of 0.4–1.4 cm s^{-1}, in excellent agreement with the estimates commonly encountered in the literature for submicron and supermicron particulate nitrate (0.1 and 2.0 cm s^{-1}, respectively) and gaseous HNO_3 (1.0 cm s^{-1}) [*Duce et al*., 1991; *Hauglustaine et al*., 1994; *Baker et al*., 2007; *Chen et al*., 2007].

[57] In addition to allowing for an estimation of the atmospheric lifetime of nitrate, the application of the continuity equation to the diurnal variations observed in this study has also provided a unique opportunity to evaluate different assumptions regarding the quantity of $\Delta^{17}O(O_3^*)$. A comparison of the $\Delta^{17}O(NO_3^-)$ time derivatives measured in this study to output produced by constraining the continuity equation to our $\Delta^{17}O(NO_3^-)$ measurements at $\Delta^{17}O(O_3^*)$ values of 34, 41, and 48‰ (the same range discussed in section 4.1.1) indicates that a value of 41‰ yields the best agreement between the calculated and measured derivatives, regardless of the value chosen for τ (see supporting information Figure S2). The application of a $\Delta^{17}O(O_3^*)$ value of 48‰ results in a significant overestimation of the magnitude of peaks in $\Delta^{17}O(NO_3^-)$ occurring as a result of nighttime nitrate production (i.e., the amplification of the continuity equation curve as shown in Figure 9). Conversely, a $\Delta^{17}O(O_3^*)$ value of 34‰ yields exaggerated negative movement in $\Delta^{17}O(NO_3^-)$ as a result of the $OH + NO_2$ reaction during the day and underestimates the magnitude of the positive derivatives resulting from nighttime production. Proportional positive and negative movements around a baseline value (i.e., a derivative of zero) can be reproduced only when using an intermediate value of $\Delta^{17}O(O_3^*)$. These observations strongly suggest that the appropriate tropospheric $\Delta^{17}O(O_3^*)$ value is indeed in the range of (41 ± 3)‰ ($\Delta^{17}O(O_3)_{bulk} \approx 25$–29‰), an assumption that has formed the basis of quantitative atmospheric interpretations derived from isotope ratio measurements in many previous studies [*Röckmann et al*., 2001; *Michalski et al*., 2003, 2004, 2005; *Alexander et al*., 2004; *Morin et al*., 2007, 2009, 2012; *Patris et al*., 2007; *Savarino et al*., 2007; *Kunasek et al*., 2008]; furthermore, these findings lend credence to the existing measurements of ozone ^{17}O-excess reported in the literature [*Krankowsky et al*., 1995; *Johnston and Thiemens*, 1997; *Vicars et al*., 2012] and substantiate the quantitative conclusions drawn in section 4.1.1 regarding the average contributions from the N_2O_5 pathway.

4.2. Interpretation of $\delta^{15}N(NO_3^-)$ Measurements

[58] Variations in the $\delta^{15}N$ of atmospheric nitrate could plausibly be attributed to four different causes: (i) variations in the $\delta^{15}N$ value of the NO_x emission, or the "source signature;" (ii) partitioning of ^{15}N between NO and NO_2; (iii) isotopic fractionations associated with the conversion of NO_x to nitrate; or (iv) isotopic effects occurring during the transport of nitrate in the atmosphere (e.g., deposition and gas-particle partitioning of HNO_3) [*Morin et al*., 2009]. There remains a great deal of uncertainty regarding the potential quantitative impacts of these processes. Isotopic fractionations associated with the atmospheric NO_x cycle have been proposed [e.g., *Freyer*, 1991; *Freyer et al*., 1993]; however, there is very little experimental or observational evidence that supports these assertions. Isotopic fractionation during atmospheric transport is typically thought to be negligible due to the relatively short lifetime of nitrate against wet and dry deposition; therefore, it is often assumed in the literature that the $\delta^{15}N$ value of NO_x is conserved from source to sink and natural spatial and temporal variations in the $\delta^{15}N$ of atmospheric nitrate are thus typically attributed to NO_x source variability [*Freyer*, 1991; *Hastings et al*., 2003, 2009; *Elliott et al*., 2007, 2009; *Savarino et al*., 2007; *Wankel et al*., 2010; *Fang et al*., 2011].

[59] The framework commonly applied in the interpretation of atmospheric $\delta^{15}N(NO_3^-)$ values can be generalized

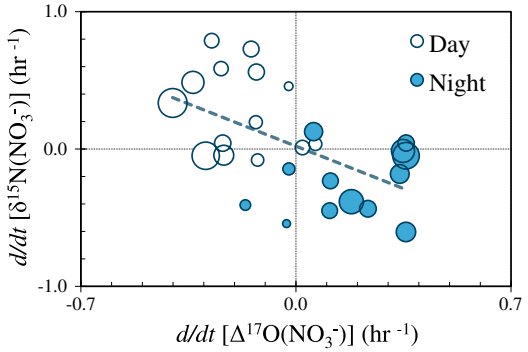

Figure 11. Bubble plot showing the time derivatives determined for $\delta^{15}N(NO_3^-)$ as a function of those determined for $\Delta^{17}O(NO_3^-)$ during the period 14–27 May. The size of the bubbles corresponds to the average atmospheric concentration of nitrate during each sampling period, which ranged from 409 to 5500 ng m^{-3}. Day-night and night-day time derivatives are indicated by open and solid bubbles, respectively.

as follows: anthropogenic NO_x emissions resulting from fuel combustion are enriched relative to atmospheric N_2. Therefore, positive $\delta^{15}N$ values in atmospheric nitrate are often taken to represent a combustion source signal. For example, *Elliott et al*. [2009] observed a strong spatial correlation between the $\delta^{15}N$ of nitrate in atmospheric dry deposition, which averaged 3.2‰, and the magnitude of NO_x emissions from stationary sources (e.g., power plants) in the eastern U.S. In another study, *Fang et al*. [2011] used $\delta^{15}N$ measurements of precipitation nitrate, which averaged 3.6‰ over a 2 year period, to estimate the relative contributions of nitrate originating from fossil fuel NO_x emissions at an industrialized site in China. Lower atmospheric $\delta^{15}N(NO_3^-)$ values, such as those reported by *Baker et al*. [2007] and *Morin et al*. [2009] for the remote Atlantic MBL (−6–0‰), are generally assumed to indicate a mostly natural background NO_x source, such as emission from soils ($\delta^{15}N < -20$‰) [*Freyer*, 1991] or production during lighting strikes ($\delta^{15}N \sim 0$) [*Hoering*, 1957].

[60] It is difficult to reconcile our observations of $\delta^{15}N(NO_3^-)$ to the commonly applied interpretive framework discussed above. Considering the large variations often observed between subsequent daytime and nighttime samples (7–10‰), it would seem that $\delta^{15}N(NO_3^-)$ was largely driven by diurnal variations associated with photochemical NO_x cycling rather than source variability. Furthermore, the only sustained periods of relative stability in $\delta^{15}N$ occurred during the nitrate concentration maxima observed under sea breeze / land breeze recirculation in the Los Angeles metropolitan region on 14–18 May and 30 May–2 June, when $\delta^{15}N(NO_3^-)$ averaged (−3.2 ± 1.4)‰ and (−2.3 ± 1.1)‰, respectively. If it can be assumed that the nitrate budget was most impacted by anthropogenic emissions during these periods (see section 4.1.2), the observation of negative $\delta^{15}N(NO_3^-)$ values seems to be inconsistent with studies that have found atmospheric nitrate derived from anthropogenic sources to possess a significantly higher $\delta^{15}N$ value than that derived from natural sources [*Elliott et al*., 2009; *Morin et al*., 2009]. However, this apparent contradiction can be resolved by considering the two main classes of combustion-related NO_x emissions: "fuel" NO_x, which is produced directly through the release and subsequent oxidation of fuel-bound nitrogen, and "thermal" NO_x, which is produced via high-temperature oxidation of O_2 and N_2 gas in combustion air, are known to possess different $\delta^{15}N$ signatures. For example, *Heaton* [1990] and *Snape et al*. [2003] obtained relatively high $\delta^{15}N$ values (6–18‰) for fuel NO_x derived from coal combustion and negative values for thermal NO_x. The production of anthropogenic NO_x proceeds through both of these processes and their relative importance determines the $\delta^{15}N$ of the NO_x produced. Coal-fired energy production has been shown to result in positive $\delta^{15}N(NO_x)$ values [*Elliott et al*., 2009; *Fang et al*., 2011; *Felix et al*., 2012]; however, there is some indication that the $\delta^{15}N$ signature of NO_x derived from transport fuel combustion is negative and can induce negative $\delta^{15}N(NO_3^-)$ values in the atmosphere [*Hastings et al*., 2003, 2009; *Widory*, 2007]. *Heaton* [1990] determined the $\delta^{15}N$ of NO_x in vehicle exhaust and obtained values ranging from −2‰ for vehicles carrying heavy loads to −13‰ for idling engines. It should be noted that there are some conflicting reports regarding the $\delta^{15}N$ of road-traffic NO_x from dendrological studies near motorways [*Ammann et al*., 1999; *Saurer et al*., 2004]; however, it seems that there is good evidence that transport fuel combustion leads to a large relative proportion of thermal NO_x production in some cases. Therefore, we tentatively conclude that the atmospheric nitrate concentration peaks occurring during the periods 14–17 May and 29–31 May were induced by emissions from vehicles and other sources of thermal NO_x in the Los Angeles metropolitan region. This conclusion is consistent with air pollution inventories prepared by the California Air Resources Board, which attribute over 50% of all NO_x emissions in the South Coast air basin to on-road motor vehicles [*CARB*, 2009]. Furthermore, there is presently very little coal combustion in California relative to the eastern U.S. However, we acknowledge that the $\delta^{15}N$ of NO_x from vehicle emissions cannot be fully resolved by the present study and identify this as an important topic for future research.

4.2.1. Diurnal Variations in $\delta^{15}N(NO_3^-)$

[61] The diurnal features of the $\delta^{15}N(NO_3^-)$ record can be summarized by considering the time derivatives determined for $\delta^{15}N(NO_3^-)$ as a function of those determined for $\Delta^{17}O(NO_3^-)$ during the period 14–27 May, as is shown in Figure 11. The largest daily variations in $\Delta^{17}O$ occurred in conjunction with maximum atmospheric nitrate concentrations, while diurnal variations in $\delta^{15}N$ were primarily restricted to periods of low or stable concentrations (i.e., significant variations in both $\Delta^{17}O$ and $\delta^{15}N$ were rarely observed in the same sample sets); thus, the correlation between these two variables is rather weak ($r = 0.54$). However, the general relationship between $\delta^{15}N$ and $\Delta^{17}O$ is unambiguous from inspection of Figure 11: nitrate produced during the night is clearly associated with positive derivatives in $\Delta^{17}O$ and negative derivatives in $\delta^{15}N$ and vice versa. From a purely phenomenological perspective, this relationship suggests the possibility of opposing kinetic isotopic effects associated with the OH and N_2O_5 pathways, which have been previously proposed by *Freyer* [1991]. However, we can reject this hypothesis in the present case based on three lines of reasoning: (i) the fractionation effects proposed by *Freyer et al*. [1991] would suggest an opposite diurnal trend

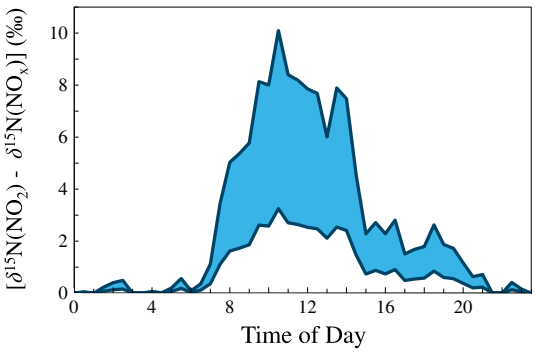

Figure 12. The diurnally averaged trend in [δ^{15}N(NO_2)–δ^{15}N(NO_x)] calculated using the O_3 and NO_x mixing ratios determined in situ and equations (11) and (12). The shaded surface represents estimates computed over a range of K values (1.022 to 1.046) for the isotopic exchange between NO and NO_2.

to that observed here (i.e., negative fractionation from the OH channel and positive fractionation from N_2O_5 hydrolysis); (ii) nitrate produced through the OH and N_2O_5 pathways was detected in different size fractions in this study (Section 4.1.2), while δ^{15}N exhibited no apparent trend with respect to particle size (Figure 7), suggesting that the isotopic effects inducing diurnal variations in δ^{15}N occurred within the NO_x pool prior to conversion to nitrate; and (iii) as previously mentioned, large diurnal variations in δ^{15}N and Δ^{17}O did not occur simultaneously and exhibited opposite trends with respect to atmospheric nitrate concentration.

[62] If the diurnal variations observed in the δ^{15}N(NO_3^-) record cannot be attributed to NO_x source variability or fractionation effects associated with NO_x to nitrate conversion, then it stands to reason that they result from either ^{15}N partitioning within NO_x or isotopic effects occurring during atmospheric transport. Given the short time scale of these variations (~12 h) and their apparent insensitivity to particle size, isotopic effects from transport (e.g., depositional effects) can almost certainly be ruled out. However, isotopic exchange between NO and NO_2, which is known to promote ^{15}N enrichment in the more oxidized form [*Sharma et al.*, 1970], is capable of explaining our observations. This isotopic partitioning proceeds through the formation and subsequent disassociation of N_2O_3 and occurs wherever NO and NO_2 coexist. The effective isotopic exchange constant (K') for this reaction was originally defined for standard tropospheric conditions by *Freyer et al.* [1993] as follows:

$$K' = \frac{[NO_x] \times k^+ + \frac{1}{\chi NO_2} \times [O_3] \times k_1}{[NO_x] \times k^- + \frac{1}{\chi NO_2} \times [O_3] \times k_1} \quad (11)$$

where k^+ and k^- are the forward and backward rate constants of the isotopic exchange reaction ($k^+/k^- = K$, the thermodynamic equilibrium constant), both equal to approximately 8.1×10^{-14} cm^3 molecules^{-1} s^{-1} at 298 K [*Sharma et al.*, 1970], and k_1 is the rate constant for the reaction between NO and O_3, equal to approximately 1.8×10^{-14} cm^3 molecules^{-1} s^{-1} [*Atkinson et al.*, 2004]. In plain words, equation (11) predicts that when NO and NO_2 occur in the same air mass ($\chi NO_2 < 1$), isotopic exchange will occur at a rate that is proportional to the ratio of NO_x to O_3 and inversely proportional to χNO_2. The dependence of K' on O_3 concentration arises from the photolytic cycling of NO_2, which tends to counteract the isotopic exchange and promotes isotopic equilibrium between NO_2 and NO_x; however, when concentrations of NO_x and O_3 are comparable, the rate of the isotopic exchange is significant and NO_2 becomes enriched in ^{15}N. The photochemical steady state operates only during daytime hours, and thus, the isotopic exchange between NO and NO_2 faces no opposing effect during the night; however, in regions that are remote from NO_x sources, the NO pool is normally titrated completely to NO_2 during the night and the isotopic exchange becomes insignificant as χNO_2 approaches 1. The overall quantitative effect of the isotopic exchange in terms of the δ^{15}N of NO_2 over that of the total NO_x reservoir, denoted [δ^{15}N(NO_2)–δ^{15}N(NO_x)], can be assessed as follows:

$$\left[\delta^{15}N(NO_2) - \delta^{15}N(NO_x)\right] = \left(K' - 1\right) \times (1 - \chi NO_2) \quad (12)$$

[63] By applying 30 min averages of the [O_3], [NO_x], and χNO_2 values determined in situ to equation (11), we have computed the diurnally averaged trend in [δ^{15}N(NO_2)–δ^{15}N(NO_x)] over the entire period of this study (Figure 12). The value of the thermodynamic equilibrium constant, K, which sets the quantitative upper limit for the isotopic exchange, is not presently well constrained. For example, *Freyer et al.* [1993] determined $K = 1.022$ in a study of NO_x in the ambient troposphere over the German city of Jülich, while other authors have determined higher values from both ad hoc calculations and direct measurements. Considering the uncertainty in this parameter, we have computed K' over the range of K values reported in the literature (1.022 to 1.046) [*Begun and Melton*, 1956; *Begun and Fletcher*, 1960; *Richet et al.*, 1977].

[64] From inspection of Figure 12, it is clear that the isotopic exchange between NO and NO_2 would have been capable of producing a qualitatively similar trend to that observed for δ^{15}N(NO_3^-) during the cruise on R/V *Atlantis*. During daytime hours, NO_x was normally present at a sufficiently high concentration relative to O_3 for isotopic exchange to lead to a significant increase in the δ^{15}N of NO_2 over that of the total NO_x pool. Therefore, nitrate production through the OH + NO_2 channel would have resulted in increasing δ^{15}N(NO_3^-) values during the day. However, due to the rapid loss of NO in the absence of photochemistry, χNO_2 was typically equal to 1 during nighttime hours (Figure 5) and thus the rate of isotopic exchange would have been negligible. Therefore, nocturnal nitrate production via the NO_3 radical would have resulted in decreasing δ^{15}N(NO_3^-) values as δ^{15}N(NO_2) approached δ^{15}N(NO_x). If we consider the average [O_3], [NO_x], and χNO_2 values during the South Coast segment of the cruise, we estimate average daytime [δ^{15}N(NO_2)–δ^{15}N(NO_x)] values of 2.1‰ and 4.5‰ for K values of 1.022 and 1.046, respectively. For the 27 diurnal samples collected during the period 14–27 May, δ^{15}N(NO_3^-) exhibited an average difference of 3.3‰ between daytime and nighttime collections, quantitatively consistent with our estimates of the exchange between NO and NO_2.

[65] The temporal and spatial variations observed in O_3 and NO_x concentrations during the cruise on R/V *Atlantis* are largely compatible with the role of isotopic exchange in

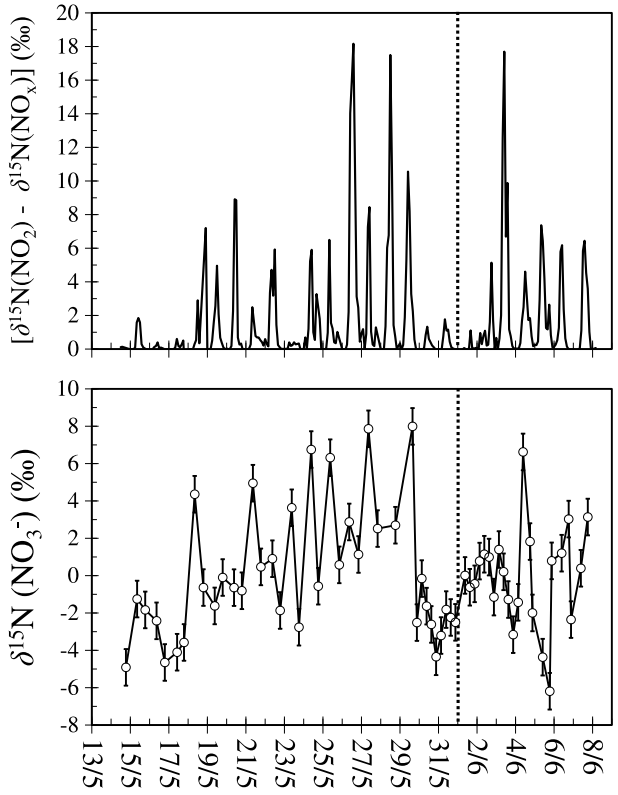

Figure 13. Spatial covariations of $[\delta^{15}N(NO_2)–\delta^{15}N(NO_x)]$ (upper panel) and $\delta^{15}N(NO_3^-)$ (lower panel) during the cruise on R/V *Atlantis*. The transit between the South and the Central Coast regions of the cruise on 1 June is indicated in each panel with a vertical dotted line.

producing the variations observed in $\delta^{15}N(NO_3^-)$. In Figure 13, $[\delta^{15}N(NO_2)–\delta^{15}N(NO_x)]$ values calculated at $K = 1.036$ (the midpoint of the range of estimates applied in Figure 12) are shown as a time series for each 2 h period of the study and compared with the observed variations in the mass-weighted $\delta^{15}N(NO_3^-)$ values. It can be seen clearly in this figure that the largest daily fluctuations in $\delta^{15}N(NO_3^-)$, such as those observed during the period 24–29 May, occurred in conjunction with maximum $[\delta^{15}N(NO_2)–\delta^{15}N(NO_x)]$ values. Conversely, the consistently negative $\delta^{15}N(NO_3^-)$ values observed during the periods 14–18 May and 30 May–2 June are associated with sustained periods of low $[\delta^{15}N(NO_2)–\delta^{15}N(NO_x)]$ estimates. Therefore, the isotopic exchange mechanism is qualitatively consistent with both the diurnality of the observed trend in $\delta^{15}N(NO_3^-)$ and its timing and magnitude during the study period.

[66] Our conclusions regarding the role of isotopic exchange in determining the $\delta^{15}N$ of nitrate have important implications for the interpretation of this variable in the atmosphere. As previously discussed, positive $\delta^{15}N$ values in atmospheric nitrate are typically taken to reflect the source signal of NO_x derived from fuel combustion. However, in air masses where NO and NO_2 occur at sufficiently high concentrations relative to O_3 during both daytime and nighttime hours (e.g., NO_x plumes from urban sources and power plants), NO_2 may become progressively enriched in ^{15}N over the NO_x source signature, resulting in $\delta^{15}N(NO_3^-)$ values that increase continuously prior to deposition. In this case, highly positive $\delta^{15}N(NO_3^-)$ values would indeed reflect anthropogenic NO_x sources, although not for the reasons commonly assumed. Such a mechanism would be largely consistent with the observations of *Elliott et al*. [2007, 2009] regarding the spatial correlation between positive $\delta^{15}N(NO_3^-)$ values in atmospheric deposition and stationary source NO_x emissions. The impact of isotopic exchange observed in this study suggests that the $\delta^{15}N$ of atmospheric nitrate does not directly reflect a NO_x source signature in all atmospheric environments, similar to the conclusions of *Savarino et al*. [2013] regarding $\delta^{15}N(NO_3^-)$ variations in the remote marine boundary layer. $\delta^{15}N(NO_3^-)$ measurements should therefore be carefully interpreted with regards to regional atmospheric context (i.e., NO, NO_2, O_3).

5. Summary and Conclusions

[67] Nocturnal reactions involving the NO_3 radical and N_2O_5 represent important NO_x sinks leading to the formation of nitrate in the atmosphere; however, the magnitude of these sinks and their variability in different atmospheric contexts remain a significant area of uncertainty. The ^{17}O-excess ($\Delta^{17}O$) of nitrate may provide a useful tracer for the relative activities of daytime and nighttime nitrate formation mechanisms at different temporal and spatial scales; however, while the interpretive power of $\Delta^{17}O(NO_3^-)$ has been demonstrated at the seasonal scale, isotopic effects associated with diurnal changes in photochemistry are presently not well constrained. In order to address these knowledge gaps, we measured the size-resolved concentration and isotopic composition of atmospheric nitrate at a diurnal/subdiurnal resolution during a research cruise along the coast of California. This cruise was organized as a component of the CalNex 2010 field study and provided a unique opportunity to combine the isotopic analysis of atmospheric nitrate with in situ measurements of the gas-phase precursors involved in its production (O_3, NO_x, N_2O_5).

[68] Our results indicate that nocturnal processes were responsible for a significant proportion of nitrate production in air masses sampled in the South Coast region during periods of continental outflow from the Los Angeles air basin, suggesting a spatial coupling of anthropogenic emissions and nighttime chemistry. Relative contributions from the N_2O_5 pathway of 30–62% were calculated using a mass balance of the $\Delta^{17}O(NO_3^-)$ data obtained for these samples; however, these quantitative estimates are extremely sensitive to the $\Delta^{17}O(O_3^*)$ value chosen in the calculation and also rest upon assumptions regarding the importance of DMS oxidation and halogen-mediated reactions to nitrate production. The N_2O_5 channel induced a strong diurnality in the $\Delta^{17}O$ of atmospheric nitrate during these periods, which was evident for samples collected at a 12 h frequency (i.e.; daytime/nighttime comparisons); however, the observed $\Delta^{17}O(NO_3^-)$ variations were out of phase with the diurnal O_3 and N_2O_5 profiles, an effect that is attributable to the lifetime of nitrate and persistent sea breeze / land breeze recirculation in the South Coast. Sustained onshore transport lead to a disruption in the diurnal $\Delta^{17}O(NO_3^-)$ pattern by delivering fine particle nitrate with a relatively long atmospheric lifetime and low $\Delta^{17}O$ to the coastal sampling location. Samples collected under a strictly marine transport regime in the Central Coast region exhibited no diurnal trend and possessed uniformly low

$\Delta^{17}O(NO_3^-)$ values, indicating relatively insignificant nitrate contributions from nighttime chemistry. This broad spatial variability in the relative importance of nocturnal NO_x processing inferred from our isotopic measurements is largely consistent with the in situ observations of O_3, NO_x, and N_2O_5 during the cruise.

[69] Spatiotemporal dynamics in $\Delta^{17}O(NO_3^-)$ were driven largely by the coarse (> 1 μm) aerosol fraction, which is composed predominantly of sea salt in the MBL and was consistently enriched in nitrate during the South Coast segment of the cruise. In agreement with previous studies, coarse particle nitrate samples exhibited $\Delta^{17}O$ values that were considerably higher than those found in the fine fraction, suggesting that the products of the N_2O_5 pathway accumulate preferentially in the supermicron mode. This observation seems to be attributable to the heterogeneous reaction of N_2O_5 with the chloride ion, which was observed to account for a large proportion of N_2O_5 loss during the South Coast segment of the cruise [*Riedel et al*., 2012; *Wagner et al*., 2012] and led to substantial chloride depletion in sea-salt aerosol measured in the Los Angeles Basin [*Hayes et al*., 2013]. The association of high $\Delta^{17}O$ values with the coarse particle fraction indicates the potential for an isotopic effect of deposition on the bulk $\Delta^{17}O$ value of atmospheric nitrate (i.e., decreasing $\Delta^{17}O(NO_3^-)$ values with long-range transport). Such an effect could provide an explanation for the relatively low $\Delta^{17}O(NO_3^-)$ observed in marine air masses during both segments of the cruise. These observations should be integrated into atmospheric models of nitrate isotope dynamics, which could be modified to account for both the size distribution of $\Delta^{17}O(NO_3^-)$ and the atmospheric lifetimes of particles in different size fractions.

[70] The magnitude and proportionality of the diurnal variability observed for $\Delta^{17}O(NO_3^-)$ during this study was accurately reproduced by constraining a continuity equation for $\Delta^{17}O(NO_3^-)$ to our measurements. This analysis represents the first direct observational evidence for the fluctuations in $\Delta^{17}O(NO_3^-)$ that have been hypothesized to result from diurnal changes in the relative activities of nitrate production pathways [*Morin et al*., 2011]. The quantitative approach adopted in this study allowed for an estimation of the atmospheric lifetime of nitrate, which is difficult to evaluate directly in the ambient troposphere. Lifetime was estimated to vary in the range of 18 to 39 h and 2 to 5 days for nitrate in continental and marine air masses, respectively, corresponding to particle deposition velocities of 0.4–1.4 cm s^{-1}, estimates that are all in good agreement with the values typically encountered in the literature. The application of the continuity equation to the diurnal variations observed in this study also provided a unique opportunity to evaluate different quantitative assumptions regarding the ^{17}O-excess of ozone. Our analysis suggests that the appropriate value for $\Delta^{17}O(O_3^*)$ is in the range of 38–44 (41 ± 3‰), a conclusion that lends credence to the existing ambient measurements of ozone isotopes as well as the numerous studies that have adopted $\Delta^{17}O(O_3^*)$ values in this range for use in quantitative interpretations.

[71] The nitrogen isotopic composition ($\delta^{15}N$) of nitrate also exhibited a clear diurnal trend during this study, typically increasing through daytime production via the OH channel and decreasing through nocturnal production. This observation is difficult to reconcile to the traditional interpretive framework in which natural spatial and temporal variations in $\delta^{15}N(NO_3^-)$ are typically attributed to NO_x source variability. While $\delta^{15}N(NO_3^-)$ did appear to reflect the $\delta^{15}N$ signature of vehicle NO_x emissions during periods of nitrate concentration maxima, the diurnal pattern was the dominant feature of the $\delta^{15}N(NO_3^-)$ record, suggesting that isotopic effects associated with diurnal changes in the NO_x cycling exert primary control on $\delta^{15}N(NO_3^-)$ at the time scale of this study. A quantitative evaluation of the in situ O_3 and NO_x measurements suggests that this diurnal pattern can be explained by the isotopic exchange equilibrium between NO and NO_2, which would have resulted in increasing $\delta^{15}N(NO_2)$ values during the day in the air masses sampled in the South Coast due to a relatively high NO_x/O_3 ratio in the Los Angeles Basin. Therefore, our results indicate that the $\delta^{15}N$ of atmospheric nitrate does not necessarily reflect a source signature under high NO_x conditions, a finding that has important implications for the use $\delta^{15}N(NO_3^-)$ as tracer for anthropogenic NO_x emissions.

[72] **Acknowledgments.** The authors gratefully acknowledge the NOAA Air Resources Laboratory (ARL) for the provision of the HYSPLIT transport and dispersion model and READY website (http://www.arl.noaa.gov/ready.php) used in this publication. The authors would also like to thank Becky Alexander (University of Washington) and several anonymous reviewers for helpful suggestions and comments on this work. The research leading to these results has received funding from the European Community's Seventh Framework Programme (FP7/2007-2013) under grant agreement 237890. The Agence Nationale de la Recherche (ANR) is also acknowledged for its financial support through the OPALE project (contract NT09-451281). LEFE-CHAT, a scientific program of the Institut National des Sciences de l'Univers (INSU/CNRS), has also provided partial funding for this study.

References

Alexander, B., J. Savarino, K. J. Kreutz, and M. H. Thiemens (2004), Impact of preindustrial biomass-burning emissions on the oxidation pathways of tropospheric sulfur and nitrogen, *J. Geophys. Res.*, *109*, D08303, doi:10.1029/2003JD004218.

Alexander, B., M. G. Hastings, D. J. Allman, J. Dachs, J. A. Thornton, and S. A. Kunasek (2009), Quantifying atmospheric nitrate formation pathways based on a global model of the oxygen isotopic composition ($\Delta^{17}O$) of atmospheric nitrate, *Atmos. Chem. Phys.*, *9*(14), 5043–5056.

Ammann, M., R. Siegwolf, F. Pichlmayer, M. Suter, M. Saurer, and C. Brunold (1999), Estimating the uptake of traffic-derived NO_2 from ^{15}N abundance in Norway spruce needles, *Oecologia*, *118*(2), 124–131.

Andreae, M. O., and P. J. Crutzen (1997), Atmospheric aerosols: Biogeochemical sources and role in atmospheric chemistry, *Science*, *276*(5315), 1052–1058.

Arnold, J. R., and W. T. Luke (2007), Nitric acid and the origin and size segregation of aerosol nitrate aloft during BRACE 2002, *Atmos. Environ.*, *41*(20), 4227–4241.

Atkinson, R., D. L. Baulch, R. A. Cox, J. N. Crowley, R. F. Hampson, R. G. Hynes, M. E. Jenkin, M. J. Rossi, and J. Troe (2004), Evaluated kinetic and photochemical data for atmospheric chemistry: Volume I—Gas phase reactions of O_x, HO_x, NO_x and SO_x species, *Atmos. Chem. Phys.*, *4*, 1461–1738.

Baker, A. R., K. Weston, S. D. Kelly, M. Voss, P. Streu, and J. N. Cape (2007), Dry and wet deposition of nutrients from the tropical Atlantic atmosphere: Links to primary productivity and nitrogen fixation, *Deep Sea Res., Part I*, *54*(10), 1704–1720.

Bateman, A., and J. Kaiser (2010), Diurnal variations in the nitrogen and oxygen isotope composition of aerosol nitrate, EGU General Assembly, [Available at http://adsabs.harvard.edu/abs/2010EGUGA..1210724B].

Bates, T. S., P. K. Quinn, D. Coffman, J. E. Johnson, and A. M. Middlebrook (2005), Dominance of organic aerosols in the marine boundary layer over the Gulf of Maine during NEAQS 2002 and their role in aerosol light scattering, *J. Geophys. Res.*, *110*, D18202, doi:10.1029/2005JD005797.

Begun, G. M., and W. H. Fletcher (1960), Partition function ratios for molecules containing nitrogen isotopes, *J. Chem. Phys.*, *33*(4), 1083–1085.

Begun, G. M., and C. E. Melton (1956), Nitrogen isotopic fractionation between NO and NO2 and mass discrimination in mass analysis of NO2, *J. Chem. Phys.*, *25*(6), 1292–1293.

Bertram, T. H., and J. A. Thornton (2009), Toward a general parameterization of N_2O_5 reactivity on aqueous particles: The competing effects of particle liquid water, nitrate and chloride, *Atmos. Chem. Phys.*, *9*(21), 8351–8363.

Böhlke, J. K., S. J. Mroczkowski, and T. B. Coplen (2003), Oxygen isotopes in nitrate: New reference materials for ^{18}O:^{17}O:^{16}O measurements and observations on nitrate-water equilibration, *Rapid Commun. Mass Spectrom.*, *17*(16), 1835–1846.

Brand, W. A., et al. (2009), Comprehensive inter-laboratory calibration of reference materials for delta $\Delta^{18}O$ versus VSMOW using various on-line high-temperature conversion techniques, *Rapid Commun. Mass Spectrom.*, *23*(7), 999–1019.

Brenninkmeijer, C. A. M., C. Janssen, J. Kaiser, T. Röckmann, T. S. Rhee, and S. S. Assonov (2003), Isotope effects in the chemistry of atmospheric trace compounds, *Chem. Rev.*, *103*(12), 5125–5161.

Brown, S. S., et al. (2004), Nighttime removal of NO_x in the summer marine boundary layer, *Geophys. Res. Lett.*, *31*, L07108, doi:10.1029/2004GL019412.

Brown, S. S., et al. (2005), Aircraft observations of daytime NO_3 and N_2O_5 and their implications for tropospheric chemistry, *J. Photochem. Photobiol., A*, *176*(1–3), 270–278.

Brown, S. S. et al. (2006), Variability in nocturnal nitrogen oxide processing and its role in regional air quality, *Science*, *311*(5757), 67–70.

California Air Resources Board (CARB) (2009), Emission data by region (Statewide), California Air Resources Board. [Available at http://www.arb.ca.gov/ei/emissiondata.htm].

Casciotti, K. L., D. M. Sigman, M. G. Hastings, J. K. Böhlke, and A. Hilkert (2002), Measurement of the oxygen isotopic composition of nitrate in seawater and freshwater using the denitrifier method, *Anal. Chem.*, *74*(19), 4905–4912.

Cass, G. R., and F. H. Shair (1984), Sulfate accumulation in a sea breeze land breeze circulation system, *J. Geophys. Res.*, *89*(D1), 1429–1438.

Chang, W. L., P. V. Bhave, S. S. Brown, N. Riemer, J. Stutz, and D. Dabdub (2011), Heterogeneous atmospheric chemistry, ambient measurements, and model calculations of N_2O_5: A review, *Aerosol Sci. Technol.*, *45*(6), 665–695.

Chen, Y., S. Mills, J. Street, D. Golan, A. Post, M. Jacobson, and A. Paytan (2007), Estimates of atmospheric dry deposition and associated input of nutrients to Gulf of Aqaba seawater, *J. Geophys. Res.*, *112*, D04309, doi:10.1029/2006JD007858.

Costa, A. W., G. Michalski, A. J. Schauer, B. Alexander, E. J. Steig, and P. B. Shepson (2011), Analysis of atmospheric inputs of nitrate to a temperate forest ecosystem from $\Delta^{17}O$ isotope ratio measurements, *Geophys. Res. Lett.*, *38*, L15805, doi:10.1029/2011GL047539.

Crutzen, P. J. (1970), Influence of nitrogen oxides on atmospheric ozone content, *Q. J. R. Meteorol. Soc.*, *96*(408), 320–325.

Draxier, R. R., and G. D. Hess (1998), An overview of the HYSPLIT 4 modelling system for trajectories, dispersion and deposition, *Aust. Meteorol. Mag.*, *47*(4), 295–308.

Dubey, M. K., R. Mohrschladt, N. M. Donahue, and J. G. Anderson (1997), Isotope specific kinetics of hydroxyl radical (OH) with water (H_2O): Testing models of reactivity and atmospheric fractionation, *J. Phys. Chem.*, *101*(8), 1494–1500.

Duce, R. A., et al. (1991), The atmospheric input of trace species to the world ocean, *Global Biogeochem. Cycles*, *5*(3), 193–259.

Ehhalt, D. H., and F. Rohrer (2000), Dependence of the OH concentration on solar UV, *J. Geophys. Res.*, *105*(D3), 3,565–3,571.

Elliott, E. M., C. Kendall, S. D. Wankel, D. A. Burns, E. W. Boyer, K. Harlin, D. J. Bain, and T. J. Butler (2007), Nitrogen isotopes as indicators of NO_x source contributions to atmospheric nitrate deposition across the midwestern and northeastern United States, *Environ. Sci. Technol.*, *41*(22), 7661–7667.

Elliott, E. M., C. Kendall, E. W. Boyer, D. A. Burns, G. G. Lear, H. E. Golden, K. Harlin, A. Bytnerowicz, T. J. Butler, and R. Glatz (2009), Dual nitrate isotopes in dry deposition: Utility for partitioning NO_x source contributions to landscape nitrogen deposition, *J. Geophys. Res.*, *114*, G04020, doi:10.1029/2008JG000889.

Erbland, J., W. C. Vicars, J. Savarino, S. Morin, M. M. Frey, D. Frosini, E. Vince, and J. M. F. Martins (2013), Air-snow transfer of nitrate on the East Antarctic plateau—Part 1: Isotopic evidence for a photolytically driven dynamic equilibrium, *Atmos. Chem. Phys.*, *13*, 6403–6419, doi:10.5194/acpd-13-6403-2013.

Fang, Y. T., K. Koba, X. M. Wang, D. Z. Wen, J. Li, Y. Takebayashi, X. Y. Liu, and M. Yoh (2011), Anthropogenic imprints on nitrogen and oxygen isotopic composition of precipitation nitrate in a nitrogen-polluted city in southern China, *Atmos. Chem. Phys.*, *11*(3), 1313–1325.

Felix, J. D., E. M. Elliott, and S. L. Shaw (2012), Nitrogen isotopic composition of coal-fired power plant NO_x: Influence of emission controls and implications for global emission inventories, *Environ. Sci. Technol.*, *46*(6), 3528–3535.

Fenn, M. E., et al. (2003), Ecological effects of nitrogen deposition in the western United States, *Bioscience*, *53*(4), 404–420.

Finlayson-Pitts, B. J., M. J. Ezell, and J. N. Pitts (1989), Formation of chemically active chlorine compounds by reactions of atmospheric NaCl particles with gaseous N_2O_5 and $ClONO_2$, *Nature*, *337*(6204), 241–244.

Frey, M. M., J. Savarino, S. Morin, J. Erbland, and J. M. F. Martins (2009), Photolysis imprint in the nitrate stable isotope signal in snow and atmosphere of East Antarctica and implications for reactive nitrogen cycling, *Atmos. Chem. Phys.*, *9*(22), 8681–8696.

Freyer, H. D. (1991), Seasonal variation of $^{15}N/^{14}N$ ratios in atmospheric nitrate species, *Tellus, Ser. B*, *43B*(1), 30–44.

Freyer, H. D., D. Kley, A. Volzthomas, and K. Kobel (1993), On the interaction of isotopic exchange processes with photochemical reactions in atmospheric oxides of nitrogen, *J. Geophys. Res.*, *98*(D8), 14,791–14,796.

Gentner, D. R., R. A. Harley, A. M. Miller, and A. H. Goldstein (2009), Diurnal and seasonal variability of gasoline-related volatile organic compound emissions in Riverside, California, *Environ. Sci. Technol.*, *43*(12), 4,247–4,252.

von Glasow, R., R. von Kuhlmann, M. G. Lawrence, U. Platt, and P. J. Crutzen (2004), Impact of reactive bromine chemistry in the troposphere, *Atmos. Chem. Phys.*, *4*, 2481–2497.

Hastings, M. G., D. M. Sigman, and F. Lipschultz (2003), Isotopic evidence for source changes of nitrate in rain at Bermuda, *J. Geophys. Res.*, *108*(D24), 4790, doi:10.1029/2003JD003789.

Hastings, M. G., J. C. Jarvis, and E. J. Steig (2009), Anthropogenic impacts on nitrogen isotopes of ice-core nitrate, *Science*, *324*(5932), 1288.

Hauglustaine, D. A., C. Granier, G. P. Brasseur, and G. Megie (1994), The importance of atmospheric chemistry in the calculation of radiative forcing on the climate system, *J. Geophys. Res.*, *99*(D1), 1,173–1,186.

Hayes, P. L., et al. (2013), Organic aerosol composition and sources in Pasadena, California during the 2010 CalNex campaign, *J. Geophys. Res. Atmos.*, doi:10.1002/jgrd.50530, in press.

Heaton, T. H. E. (1990), 15N/14N ratios of NOx from vehicle engines and coal-fired power stations, *Tellus, Ser. B*, *42*, 304–307, doi:10.1034/j.1600-0889.1990.00007.x-i1.

Hoering, T. (1957), The isotopic composition of the ammonia and the nitrate ion in rain, *Geochim. Cosmochim. Acta*, *12*(1–2), 97–102.

Holland, E. A., et al. (1997), Variations in the predicted spatial distribution of atmospheric nitrogen deposition and their impact on carbon uptake by terrestrial ecosystems, *J. Geophys. Res.*, *102*(D13), 15,849–15,866.

Jaegle, L., L. Steinberger, R. V. Martin, and K. Chance (2005), Global partitioning of NOx sources using satellite observations: Relative roles of fossil fuel combustion, biomass burning and soil emissions, *Faraday Discuss.*, *130*, 407–423.

Jarvis, J. C., E. J. Steig, M. G. Hastings, and S. A. Kunasek (2008), Influence of local photochemistry on isotopes of nitrate in Greenland snow, *Geophys. Res. Lett.*, *35*, L21804, doi:10.1029/2008GL035551.

Johnston, J. C., and M. H. Thiemens (1997), The isotopic composition of tropospheric ozone in three environments, *J. Geophys. Res.*, *102*(D21), 25,395–25,404.

Kaiser, J., M. G. Hastings, B. Z. Houlton, T. Röckmann, and D. M. Sigman (2007), Triple oxygen isotope analysis of nitrate using the denitrifier method and thermal decomposition of N_2O, *Anal. Chem.*, *79*(2), 599–607.

Krankowsky, D., F. Bartecki, G. G. Klees, K. Mauersberger, K. Schellenbach, and J. Stehr (1995), Measurement of heavy isotope enrichment in tropospheric ozone, *Geophys. Res. Lett.*, *22*(13), 1713–1716.

Kunasek, S. A., B. Alexander, E. J. Steig, M. G. Hastings, D. J. Gleason, and J. C. Jarvis (2008), Measurements and modeling of $\Delta^{17}O$ of nitrate in snowpits from Summit, Greenland, *J. Geophys. Res.*, 113, D24302, doi:10.1029/2008JD010103.

Lerner, B. M., P. C. Murphy, and E. J. Williams (2009), Field measurements of small marine craft gaseous emission factors during NEAQS 2004 and TexAQS 2006, *Environ. Sci. Technol.*, *43*(21), 8213–8219.

Liang, J. Y., L. W. Horowitz, D. J. Jacob, Y. H. Wang, A. M. Fiore, J. A. Logan, G. M. Gardner, and J. W. Munger (1998), Seasonal budgets of reactive nitrogen species and ozone over the United States, and export fluxes to the global atmosphere, *J. Geophys. Res.*, *103*(D11), 13,435–13,450.

Likens, G. E., C. T. Driscoll, and D. C. Buso (1996), Long-term effects of acid rain: Response and recovery of a forest ecosystem, *Science*, *272*(5259), 244–246.

Lu, R., and R. P. Turco (1994), Air pollutant transport in a coastal environment – Part 1: 2-dimensional simulations of sea-breeze and mountain effects, *J. Atmos. Sci.*, *51*(15), 2285–2308.

Lu, R., and R. P. Turco (1995), Air pollutant transport in a coastal environment – Part 2: 3-dimensional simulations over Los Angeles basin, *Atmos. Environ.*, *29*(13), 1499–1518.

Lyons, J. R. (2001), Transfer of mass-independent fractionation in ozone to other oxygen-containing radicals in the atmosphere, *Geophys. Res. Lett.*, *28*(17), 3231–3234.

Malm, W. C., B. A. Schichtel, M. L. Pitchford, L. L. Ashbaugh, and R. A. Eldred (2004), Spatial and monthly trends in speciated fine particle concentration in the United States, *J. Geophys. Res.*, *109*, D03306, doi:10.1029/2003JD003739.

McCabe, J. R., M. H. Thiemens, and J. Savarino (2007), A record of ozone variability in South Pole Antarctic snow: Role of nitrate oxygen isotopes, *J. Geophys. Res.*, *112*, D12303, doi:10.1029/2006JD007822.

McLaren, R., P. Wojtal, D. Majonis, J. McCourt, J. D. Halla, and J. Brook (2010), NO3 radical measurements in a polluted marine environment: Links to ozone formation, *Atmos. Chem. Phys.*, *10*(9), 4187–4206.

Michalski, G., J. Savarino, J. K. Böhlke, and M. Thiemens (2002), Determination of the total oxygen isotopic composition of nitrate and the calibration of a $\Delta^{17}O$ nitrate reference material, *Anal. Chem.*, *74*(19), 4989–4993.

Michalski, G., Z. Scott, M. Kabiling, and M. H. Thiemens (2003), First measurements and modeling of $\Delta^{17}O$ in atmospheric nitrate, *Geophys. Res. Lett.*, *30*(16), 1870, doi:10.1029/2003GL017015.

Michalski, G., J. K. Bohlke, and M. Thiemens (2004), Long term atmospheric deposition as the source of nitrate and other salts in the Atacama Desert, Chile: New evidence from mass-independent oxygen isotopic compositions, *Geochim. Cosmochim. Acta*, *68*(20), 4023–4038.

Michalski, G., J. G. Bockheim, C. Kendall, and M. Thiemens (2005), Isotopic composition of Antarctic Dry Valley nitrate: Implications for NO_y sources and cycling in Antarctica, *Geophys. Res. Lett.*, *32*, L13817, doi:10.1029/2004GL022121.

Millet, D. B., et al. (2004), Volatile organic compound measurements at Trinidad Head, California, during ITCT 2K2: Analysis of sources, atmospheric composition, and aerosol residence times, *J. Geophys. Res.*, *109*, D23S16, doi:10.1029/2003JD004026.

Monks, P. S. (2005), Gas-phase radical chemistry in the troposphere, *Chem. Soc. Rev.*, *34*(5), 376–395.

Morin, S., J. Savarino, S. Bekki, S. Gong, and J. W. Bottenheim (2007), Signature of Arctic surface ozone depletion events in the isotope anomaly ($\Delta^{17}O$) of atmospheric nitrate, *Atmos. Chem. Phys.*, *7*, 1451–1469.

Morin, S., J. Savarino, M. M. Frey, N. Yan, S. Bekki, J. W. Bottenheim, and J. M. F. Martins (2008), Tracing the origin and fate of NO_x in the arctic atmosphere using stable isotopes in nitrate, *Science*, *322*(5902), 730–732.

Morin, S., J. Savarino, M. M. Frey, F. Domine, H. W. Jacobi, L. Kaleschke, and J. M. F. Martins (2009), Comprehensive isotopic composition of atmospheric nitrate in the Atlantic Ocean boundary layer from 65 degrees S to 79 degrees N, *J. Geophys. Res.*, *114*, D05303, doi:10.1029/2008JD010696.

Morin, S., R. Sander, and J. Savarino (2011), Simulation of the diurnal variations of the oxygen isotope anomaly ($\Delta^{17}O$) of reactive atmospheric species, *Atmos. Chem. Phys.*, *11*(8), 3653–3671.

Morin, S., J. Erbland, J. Savarino, F. Domine, J. Bock, U. Friess, H. W. Jacobi, H. Sihler, and J. M. F. Martins (2012), An isotopic view on the connection between photolytic emissions of NO_x from the Arctic snowpack and its oxidation by reactive halogens, *J. Geophys. Res.*, *117*, D00R08, doi:10.1029/2011JD016618.

Osthoff, H. D., et al. (2008), High levels of nitryl chloride in the polluted subtropical marine boundary layer, *Nat. Geosci.*, *1*(5), 324–328.

Parrella, J. P., et al. (2012), Tropospheric bromine chemistry: Implications for present and pre-industrial ozone and mercury, *Atmos. Chem. Phys.*, *12*(15), 6723–6740.

Patey, M. D., M. J. A. Rijkenberg, P. J. Statham, M. C. Stinchcombe, E. P. Achterberg, and M. Mowlem (2008), Determination of nitrate and phosphate in seawater at nanomolar concentrations, *Trends Anal. Chem.*, *27*(2), 169–182.

Patris, N., S. S. Cliff, P. K. Quinn, M. Kasem, and M. H. Thiemens (2007), Isotopic analysis of aerosol sulfate and nitrate during ITCT-2k2: Determination of different formation pathways as a function of particle size, *J. Geophys. Res.*, *112*, D23301, doi:10.1029/2005JD006214.

Phillips, G. J., M. J. Tang, J. Thieser, B. Brickwedde, G. Schuster, B. Bohn, J. Lelieveld, and J. N. Crowley (2012), Significant concentrations of nitryl chloride observed in rural continental Europe associated with the influence of sea salt chloride and anthropogenic emissions, *Geophys. Res. Lett.*, *39*, L10811, doi:10.1029/2012GL051912.

Platt, U., and G. Honninger (2003), The role of halogen species in the troposphere, *Chemosphere*, *52*(2), 325–338.

Prospero, J. M., and D. L. Savoie (1989), Effect of continental sources on nitrate concentrations over the Pacific Ocean, *Nature*, *339*(6227), 687–689.

Richet, P., Y. Bottinga, and M. Javoy (1977), Review of hydrogen, carbon, nitrogen, oxygen, sulfur, and chlorine stable isotope fractionation among gaseous molecules, *Annu. Rev. Earth Planet. Sci.*, *5*, 65–110.

Riedel, T. P., et al. (2012), Nitryl chloride and molecular chlorine in the coastal marine boundary layer, *Environ. Sci. Technol.*, *46*(19), 10,463–10,470.

Röckmann, T., J. Kaiser, J. N. Crowley, C. A. M. Brenninkmeijer, and P. J. Crutzen (2001), The origin of the anomalous or "mass-independent" oxygen isotope fractionation in tropospheric N_2O, *Geophys. Res. Lett.*, *28*(3), 503–506.

Russell, K. M., J. N. Galloway, S. A. Macko, J. L. Moody, and J. R. Scudlark (1998), Sources of nitrogen in wet deposition to the Chesapeake Bay region, *Atmos. Environ.*, *32*(14–15), 2453–2465.

Ryerson, T. B., et al. (2013), The 2010 California Research at the Nexus of Air Quality and Climate Change (CalNex) field study, *J. Geophys. Res. Atmos.*, *118*, 5830–5866, doi:10.1002/jgrd.50331.

Sander, R., Y. Rudich, R. von Glasow, and P. J. Crutzen (1999), The role of $BrNO_3$ in marine tropospheric chemistry: A model study, *Geophys. Res. Lett.*, *26*(18), 2857–2860.

Sarwar, G., H. Simon, P. Bhave, and G. Yarwood (2012), Examining the impact of heterogeneous nitryl chloride production on air quality across the United States, *Atmos. Chem. Phys.*, *12*(14), 6455–6473.

Saurer, M., P. Cherubini, M. Ammann, B. De Cinti, and R. Siegwolf (2004), First detection of nitrogen from NO_x in tree rings: A $^{15}N/^{14}N$ study near a motorway, *Atmos. Environ.*, *38*(18), 2779–2787.

Savarino, J., and M. H. Thiemens (1999), Mass-independent oxygen isotope (^{16}O, ^{17}O, ^{18}O) fractionation found in H_x, O_x reactions, *J. Phys. Chem.*, *103*(46), 9221–9229.

Savarino, J., J. Kaiser, S. Morin, D. M. Sigman, and M. H. Thiemens (2007), Nitrogen and oxygen isotopic constraints on the origin of atmospheric nitrate in coastal Antarctica, *Atmos. Chem. Phys.*, *7*(8), 1925–1945.

Savarino, J., S. Morin, J. Erbland, F. Grannec, M. D. Patey, W. C. Vicars, B. Alexander, and E. P. Achterberg (2013), Isotopic composition of atmospheric nitrate in a tropical marine boundary layer, *Proc. Natl. Acad. Sci. U. S. A.*, doi:10.1073/pnas.1216639110, in press.

Sharma, H. D., R. E. Jervis, and K. Y. Wong (1970), Isotopic exchange reactions in nitrogen oxides, *J. Phys. Chem.*, *74*(4), 923–933.

Sigman, D. M., K. L. Casciotti, M. Andreani, C. Barford, M. Galanter, and J. K. Böhlke (2001), A bacterial method for the nitrogen isotopic analysis of nitrate in seawater and freshwater, *Anal. Chem.*, *73*(17), 4145–4153.

Snape, C. E., C. G. Sun, A. E. Fallick, R. Irons, and J. Haskell (2003), Potential of stable nitrogen isotope ratio measurements to resolve fuel and thermal NO_x in coal combustion, *Prepr. Am. Chem. Soc. Div. Fuel Chem.*, *48*(1), 3–5.

Sommariva, R., et al. (2009), Radicals in the marine boundary layer during NEAQS 2004: a model study of day-time and night-time sources and sinks, *Atmos. Chem. Phys.*, *9*(9), 3075–3093.

Stark, H., S. S. Brown, P. D. Goldan, M. Aldener, W. C. Kuster, R. Jakoubek, F. C. Fehsenfeld, J. Meagher, T. S. Bates, and A. R. Ravishankara (2007), Influence of nitrate radical on the oxidation of dimethyl sulfide in a polluted marine environment, *J. Geophys. Res.*, *112*, D10S10, doi:10.1029/2006JD007669.

Stutz, J., K. Hebestreit, B. Alicke, and U. Platt (1999), Chemistry of halogen oxides in the troposphere: Comparison of model calculations with recent field data, *J. Atmos. Chem.*, *34*(1), 65–85.

Thiemens, M. H. (1999), Mass-independent isotope effects in planetary atmospheres and the early solar system, *Science*, *283*(5400), 341–345.

Thiemens, M. H. (2006), History and applications of mass-independent isotope effects, *Annu. Rev. Earth Planet. Sci.*, *34*, 217–262.

Thornton, J. A., et al. (2010), A large atomic chlorine source inferred from mid-continental reactive nitrogen chemistry, *Nature*, *464*(7286), 271–274.

Vicars, W. C., S. K. Bhattacharya, J. Erbland, and J. Savarino (2012), Measurement of the ^{17}O-excess ($\Delta^{17}O$) of tropospheric ozone using a nitrite-coated filter, *Rapid Commun. Mass Spectrom.*, *26*(10), 1219–1231.

Virkkula, A., K. Teinila, R. Hillamo, V. Matti-Kerminen, S. Saarikoski, M. Aurela, I. K. Koponen, and M. Kulmala (2006), Chemical size distributions of boundary layer aerosol over the Atlantic Ocean and at an Antarctic site, *J. Geophys. Res.*, *111*, D05306, doi:10.1029/2004JD004958.

Wagner, N. L., W. P. Dube, R. A. Washenfelder, C. J. Young, I. B. Pollack, T. B. Ryerson, and S. S. Brown (2011), Diode laser-based cavity ring-down instrument for NO_3, N_2O_5, NO, NO_2 and O_3 from aircraft, *Atmos. Meas. Tech.*, *4*(6), 1227–1240.

Wagner, N. L., et al. (2012), The sea breeze/land breeze circulation in Los Angeles and its influence on nitryl chloride production in this region, *J. Geophys. Res.*, *117*, D00V24, doi:10.1029/2012JD017810.

Wankel, S. D., Y. Chen, C. Kendall, A. F. Post, and A. Paytan (2010), Sources of aerosol nitrate to the Gulf of Aqaba: Evidence from $\Delta^{15}N$ and $\delta^{18}O$ of nitrate and trace metal chemistry, *Mar. Chem.*, *120*(1–4), 90–99.

Widory, D. (2007), Nitrogen isotopes: Tracers of origin and processes affecting PM10 in the atmosphere of Paris, *Atmos. Environ.*, *41*(11), 2382–2390.

Williams, E. J., F. C. Fehsenfeld, B. T. Jobson, W. C. Kuster, P. D. Goldan, J. Stutz, and W. A. McCleanny (2006), Comparison of ultraviolet absorbance, chemiluminescence, and DOAS instruments for ambient ozone monitoring, *Environ. Sci. Technol.*, *40*(18), 5755–5762.

Wood, R., and C. S. Bretherton (2004), Boundary layer depth, entrainment, and decoupling in the cloud-capped subtropical and tropical marine boundary layer, *J. Clim.*, *17*(18), 3576–3588.

Yeatman, S. G., L. J. Spokes, P. F. Dennis, and T. D. Jickells (2001), Can the study of nitrogen isotopic composition in size-segregated aerosol nitrate and ammonium be used to investigate atmospheric processing mechanisms?, *Atmos. Environ.*, *35*(7), 1337–1345.

Zahn, A., P. Franz, C. Bechtel, J. U. Grooss, and T. Röckmann (2006), Modelling the budget of middle atmospheric water vapour isotopes, *Atmos. Chem. Phys.*, *6*, 2073–2090.